Optimize the Efficiency of Smectites in Detoxifying Aflatoxins in Animal Feeds

Final Report to

Texas Corn Producers Board

By

Youjun Deng, Ph.D.
Assistant Professor of Soil Clay Mineralogy
Department of Soil and Crop Sciences; Texas AgriLife, Texas A&M University
College Station, TX 77843-2474
Tel: (979)-862-8476; Fax: (979)-845-0456; E-mail: yjd@tamu.edu

Joe B. Dixon, Ph.D.
Emeritus Professor of Soil Clay Mineralogy
Department of Soil and Crop Sciences; Texas AgriLife, Texas A&M University
College Station, TX 77843-2474
Tel: (979) 845-8323; FAX: (979) 845-0456, Email: j-dixon@tamu.edu

Christopher A. Bailey, Ph.D.
Professor of Poultry Science and Nutritionist
Poultry Science Department; Texas AgriLife, Texas A&M University
College Station, TX 77843-2472
Tel: (979) 845-7537; Fax: (979) 845-1921; Email: c-bailey@tamu.edu

December 30, 2011

Optimize the Efficiency of Smectites in Detoxifying Aflatoxins in Animal Feeds

Youjun Deng[1], Joe B. Dixon[1], and Christopher A. Bailey[2]
[1]Department of Soil and Crop Sciences, [2]Department of Poultry Science
Texas AgriLife, Texas A&M University, College Station, TX 77843-2474

1 Executive Summary

Frequent occurrence of high levels of aflatoxins in Texas corn appears unavoidable. Implementation of practical detoxication methods is highly desirable for animal growers and for corn producers in Texas. Our research in the last few years has established the mineralogical and chemical selection criteria for high-binding capacity bentonites, has revealed aflatoxin bonding mechanisms, and has shown promising performance of the bentonites in poultry trials. This project has tacked more practical issues related to the use of clays as mycotoxin binders. In this project, we listed two major research **objectives**: 1). Maximize the affinity and selectivity of smectites for aflatoxins; and 2). Maximize adsorption site accessibility of smectite in viscous animal digestion fluids. We have finished the experiments and are in the process of data analysis and of publication preparation. For objective one, the results are in excellent agreement with our hypothesis and have enhanced our confidence on the selectivity of smectite for aflatoxin. Higher affinity and selectivity can be achieved by (1) selecting low-charge density smectites, (2) modifying the clays with high-valence and low-hydration-energy exchange cations, and (3) reducing the charge density of the clay by varying the clay's layer structural cation compositions. The results have be presented at the 2011 EuroClay Conference in June, 2011, the annual meetings of Clay Minerals Society in September, 2011 and of the Soil Science Society of America in October, 2011. An article has been published in July, 2011. A manuscript is in revision and another manuscript is in preparation based on the results. Experimental work for objective two has been finished, and we are processing the data. Two graduate students and two student worker were involved in this project. One student finished her Master degree thesis in May 2011, which is partly supported by this project.

For objective 1), we hypothesized that the high affinity and selectivity of smectites for aflatoxin can be achieved by matching the size and polarity between aflatoxin molecules and the nanometer-scale nonpolar domains on smectite surfaces. In the early phase of the project, we have used two approaches to achieve this goal and based on these findings, we added the third approach to prove it. **Approach A: Selecting smectites with adequate charge density.** We investigated the selectivity and affinity of a series of smectites that have different charge densities. These smectites were fractionated from natural bentonites and treated with same exchange cations to eliminate the exchange cation effects. After purification of the minerals with size fractionation, we have refined the charge density of the best smectites, they should have a cation exchange capacities (CEC) of about 110 cmol(+)/kg. **Approach B: Modifying smectites with different exchange cations to change the size of nano-scale domains on smectite surfaces.** We compared the affinity and capacity of smectites for aflatoxin after replacing the exchange cations with Li, Na, K, Cs, Ca, Mg, Sr, and Ba and found the the divalent-cation saturated smectites had higher affinity than the monovalent cation saturated ones. A more than 20-fold difference was observed on the same smectite's affinity for aflatoxin after the different cation exchange treatments. Moreover, saturating the exchange sites with divalent cations that have lower hydration energies resulted in the smectite's greatest affinity for aflatoxin. These observations suggest that adequate cation exchange is needed for smectites used in aflatoxin detoxification. **Approach C: Reducing the charge density of the highly-charged smectites by inserting Li cations into the vacant octahedral sites in their layer structures,** and test the modified clays' selectivity and capacity for the aflatoxin. After reducing the charge density with Approach C, the clay's adsorption capacity and affinity for aflatoxin increased. We expect these approaches can also be used to modify clays to enhance their selectivity for other mycotoxins such as

ochratoxin A, zearalenone, and deoxynivalenol.

For objective 2: We have attempted to make the interlayer space of smectite accessible to aflatoxins in stomach and intestine fluids. In this study, we tested smectite incorporation methods by using simulating gastrointestinal fluids (GF). The clays were added to the simulating fluids in the following four forms: (1) air dried powder, which is the form used in most animal trials, (2) freeze dried powder that should have much high porosity than the air dried clays, (3) diluted smectite clay suspension that was well dispersed by sonication, and (4) anionic polymer solution treated smectite suspension in which the clay dispersion was enhanced and stabilized. Our experiment has suggested that aflatoxin adsorption in GF reduced by 33% to 61% than the adsorption in water, depending on the clay's dispersion status. Difference in adsorption could be due to GF's acidic pH (4.8 in water and 3.3 in the simulated GF). Sonicated clay suspension showed the highest adsorption both in water (18.4% w/w) and GF (9.6% w/w). The polymer stabilized clay suspension and freeze dried clay were similar in adsorption in water, but in GF the freeze dry clay showed lower adsorption. Oven dry clay showed the lowest adsorption in both solutions (12.7% w/w in water and 5.3% w/w in GF). These results indicate that gastric fluid reduced the clay's aflatoxin adsorption effectiveness in acidic condition. Higher adsorption of aflatoxin in GF can be achieved by increasing clay's dispersion before they were introduced into the GF system. In general, a lower adsorption of aflatoxin on the smectites has been observed when pH of GF solution was decreased.

These observations suggest that smectites' selectivity and adsorption capacity for aflatoxin can be enhanced by matching the size and the polarity of the toxin with the adsorption sites of smectites on the nanometer scale. Biological molecules in the gastrointestinal fluids do interfere the adsorption of aflatoxin on smectites, yet, high aflatoxin binding efficiency can still be achieved when the clay particles are well dispersed. These efficiencies will be further tested in poultry trials and cytotoxicity studies in 2012.

2 Presentation Abstracts

1. Deng, Y., L. Liu, M. Szczerba, A. L. Barrientos Velazquez, and J. B. Dixon. Mineralogy factors determining bentonite effectiveness in aflatoxin detoxification. *ASA, CSSA, and SSSA 2011 International Annual Meetings.* San Antonio, Texas, USA. October 16-19. 2011.

   Frequent occurrence of aflatoxins in feed and food appear to be unavoidable. Adding bentonites to aflatoxin-contaminated feed has improved animal performance in many studies. Incorporating bentonites into human diet has also shown promising results in reducing the bioavailability of aflatoxins. Despite the encouraging results from animal and human trials, no regulatory agency has approved the use of bentonite as aflatoxin amendment agents due in part to lack of confidence and poor understanding of the detoxification mechanisms. The objectives of this study are to describe: (1) critical mineralogical properties of bentonites that determine their adsorption selectivity and capacity for aflatoxins and (2) research needs to improve the clay's detoxification effectiveness *in vivo*. Smectite in the bentonite dominates the adsorption of aflatoxin. Adsorption of aflatoxin can occur on both external surfaces and in the interlayer space of smectite. Up to 0.6 mol/kg (or 20% by mass) of aflatoxin can be adsorbed by smectites that have relatively low cation exchange capacities (about 100 cmol/kg or less). The adsorption appears to be irreversible. Only <0.5% desorption by water washing was observed. The type of exchange cation on smectite plays a critical role in determining its affinity and adsorption capacity for aflatoxin. Divalent cation saturated smectites have much higher adsorption affinity than monovalent cations. These results have led us to conclude that size and polarity match between aflatoxin molecules and the adsorbing domains are key factors in determining selectivity of the clay and binding capacity for aflatoxin. Both theoretical computation and adsorption experiments after cation exchange have supported this conclusion. Well-defined concepts and evidences are needed on the interactions between bentonites and aflatoxins *in vivo*.

2. Barrientos Velazquez, A. L., Y. Deng, C. A. Bailey, and J. B. Dixon, Enhance Aflatoxin Accessibility into Smectite in Simulated Gastric Fluids. *ASA, CSSA, and SSSA 2011 International Annual Meetings.* San Antonio, Texas, USA. October 16-19. 2011

   Corn, peanuts and other crops can be invaded by Fungi *Aspergillus flavus* and *Aspergillus parasiticus*, which produce carcinogenic aflatoxins. The regulated maximum concentration of aflatoxins in food is 20ppb and between 20 - 300ppb for animal feeds. Among the aflatoxin decontamination techniques, incorporation of adsorbents in animal diet has been extensively investigated. In vitro experiments have demonstrated high aflatoxin adsorption capacities of bentonites (up to 20% of the clay's mass), but poultry experiments showed large variations in chicken's response. The clay's in vivo effectiveness need to be enhanced. The objectives of this research were 1) to evaluate the simulated gastric fluid effect on the clay's aflatoxin adsorption capacity, and 2) to evaluate the effect of clay dispersion methods on the aflatoxin adsorption. Single point aflatoxin concentration of 4.8ppm was used to compare clay adsorption in water and simulated gastric fluid (GF). Four clay treatments were used to compare the dispersion effect: 1) oven (60 C) dried clay powder, 2) freeze dried clay powder, 3) sonicated clay suspension, and 4) anionic polymer stabilized clay suspension. Compared to the adsorption in water, aflatoxin adsorption in GF reduced by 33% to 61%, depending on the clay's dispersion status. Difference in adsorption could be due to GF's acidic pH (4.8 in water and 3.3 in the simulated GF). Sonicated clay suspension showed the highest adsorption both in water (18.4% w/w) and GF (9.6% w/w). The polymer stabilized clay suspension and freeze dried clay were similar in adsorption in water, but in GF the freeze dry clay showed lower adsorption. Oven dry clay showed the lowest adsorption in both solutions (12.7% w/w in water and 5.3% w/w in GF). These results indicate that gastric fluid reduced the clay's aflatoxin adsorption effectiveness in acidic condition. Higher

adsorption of aflatoxin can be achieved by increasing the clay dispersion.

3. Liu, L. and Y. Deng. Adsorption of aflatoxin B_1 on modified bentonite clays. *ASA, CSSA, and SSSA 2011 International Annual Meetings.* San Antonio, Texas, USA. October 16-19. 2011

   Aflatoxins are toxic metabolites produced by *Aspergillus fungi*. They are widely recognized as a contamination for grains. Among the 20 carcinogenic natural aflatoxins, aflatoxin B_1 (AfB_1) is considered the most toxic to animals and humans. Bentonite clays are used as anticaking additives in the pelletization of animal feeds. They also have shown extra benefits in reducing the concentration of AfB1 by adsorption. The major mineralogical and chemical properties of bentonites in determining their adsorption capacities for AfB1 are still poorly understood, which limits the selection, modification, and application of the clays as an aflatoxin binder. In this study, adsorption of AfB1 on clay fractions of six bentonites (referred to as 37GR, 1MS, 5OK, 7AZ, 8TX and 16MX) was investigated to determine the critical mineralogical properties as a good adsorbent. AfB_1 adsorption isotherms were fitted with Langmuir, modified Langmuir with adsorption dependent affinity, and exponential Langmuir models. The interlayer cations in 37GR were replaced with four monovalent cations (Li, Na, K, Cs) and four divalent cations (Ca, Mg, Ba, Sr). The divalent cation saturation in general resulted in much higher adsorption capacity and affinity. Cations with small hydration radii lowered the affinity and adsorption capacity of the clay for AfB_1. For all six clays, Ba saturation enhanced the size and polarity matching among clay particles, AfB1 molecules and cations, therefore increased the adsorption when compared with Ca saturation. A negative correlation was observed between cation exchange capacity and AfB_1 adsorption. The importance of size and polarity matching in the adsorption process will be further verified in charge reduction experiments.

4. Barrientos-Velázquez, A.L., A. Marroquín-Cardona, J.B. Dixon and Y. Deng. Effects of charge origin and octahedral cations of smectites on their selectivity and adsorption capacity for aflatoxin. *48th Annual Meeting of The Clay Minerals Society.* Lake Tahoe, Nevada, USA. September 24-29, 2011.

   Every year, corn, peanuts, cotton seeds, tree nuts, and a variety of crops arecontaminated by mycotoxins. The most toxic and carcinogenic mycotoxins are aflatoxins produced by fungi *Aspergillus flavus* and *Aspergilli sparasiticus*. Adding clays to animal feeds is an effective and low cost measure in reducing the bioavailability of aflatoxinsto animals. We have investigated several bentonite samples from the USA and other countries and found that their AfB1 adsorption capacity varied from 1.8 to 21.1 % (w/w). Our analysis has demonstrated that the major adsorption site for aflatoxin is the interlayer space in smectites. It appears to be critical to preserve the interlayer the accessibility of aflatoxin molecules, which can be affected by many physical and chemical properties of the samples. More recently, experiments have confirmed that the exchangeable cation strongly influences the amount of aflatoxin that can be adsorbed. It also appears that the octahedral structural cations might influence the adsorption. As the swell/shrink properties of smectites are affected by charge density and charge origin, we expect that the charge origin might influence aflatoxin adsorption. The objective of this study was todetermine the effects of the charge origin and octahedral cations on the selectivity and adsorption capacity for aflatoxin.

   Six smectite samples with different layer charge sources and octahedral type were selected. Both natural bulk materials and the clay fractions of a beidellite, ahectorite, twomontmorillonite (Novasil and 4TX), anontronite, anda saponite (Spain and Australia) samples were evaluated for their aflatoxin adsorption capacity and affinity. The maximum adsorption capacity for the unfractionated samples showed a variation among the samples. Montmorillonite 4TX had the high-

est adsorption of 0.4 mol/kg, followed by montmorilloniteNovasil with 0.35mol/kg and saponite Spain with 0.35 mol/kg. Beidellite, saponite Australia and hectorite showed and intermediate adsorption of about 0.20mol/kg. The lowest adsorbent was nontronitewith 0.17 mol/kg. The variations among the unfractionated samples appear to be determined by other minerals in the samples. The x-ray diffraction patterns showed quartz and feldspars in the samples. Additionally the saponites contained mica and hectorite calcite. The clay fraction confirmed the presence of mica in both saponites while smectite was the dominant mineral in the other samples.

Aflatox adsorption on the clay fractions are under investigating. Preliminary results suggest that the selectivity or adsorption capacity of the smectites for aflatoxin was not determined by the origin of the charge on the smectites or the type of octahedral cations, rather, the charge density of the minerals and the type of exchange cations play more important roles.

5. Deng, Y. , L. Liu, A. L. Barrientos-Velázquez, and J. B. Dixon. Smectite structural domains as a controlling factor in aflatoxin adsorption. *Euroclay 2011.* Antalya, Turkey, June 26-July 1. 2011.

   Aflatoxins are carcinogenic metabolites produced by fungi *Aspergillus flavus* and *A. parasitcus.* Occurrence of aflatoxins in cereal grains, oil seeds, food and feeds is unavoidable due to heat, drought, insects, or other biological stresses during crop growth, grain transport, or storage. Using bentonites to adsorb aflatoxin has been proved to be an effective method to minimize the toxicity of aflatoxin to animals and humans. Among many tested bentonites, only a few of them demonstrated high adsorption capacity (up to 20% of the clays' mass) for aflatoxins. It has been confirmed that it is the smectite in the clays that adsorbs aflatoxin. No singular correlation has been observed among clay mineralogical, chemical, or physical properties with aflatoxin adsorption capacity. It is unclear what factors determin the selectivity of bentonites for aflatoxin. We hypothesize that a bentonite's selectivity and adsorption capacity for aflatoxin is mainly determined by the size of nanometer-scaled nonpolar domains between hydrated exchange cations in the smectite interlayer spaces. When the size of these non-polar domains matches the size of aflatoxin, the smectite would show high selectivity and adsorption capacity for aflatoxin. We are seeking the optimum size of interlayer nanometer-scale domains by (1) selecting smectites with different charge density and (2) varying the valence and the size of exchange cations to control the amount of water in the hydration shell of the cations. High aflatoxin adsorption capacity and high selectivity for aflatoxin can be achieved by selecting smectites that have low charge density as represented by their < 80 cmol(+) kg^{-1} cation exchange capacity. An individual smectite's selectivity and adsorption capacity for aflatoxin can be enhanced or weakened by replacing the exchange cation. For example, when a Greek smectite was saturated with divalent cations that have greater radii (e.g., Ba^{2+}, Sr^{2+}), it showed a nearly six times higher adsorption capacity and affinity compared with the same smectite saturated with Li^{+}. The preliminary results confirmed the importance of nanometer scale polarity and size match between aflatoxin molecules and the adsorbing sites on smectite. High selectivity for aflatoxin can be achieved by selecting smectite with adequate charge density or by replacing the exchange cations with divalent cations that have low hydration energy.

3 Thesis Abstract

1. Barrientos-Velázquez, A.L. 2011. Texas Bentonites as Amendments of Aflatoxin-Contaminated Poultry Feed. Texas A&M University, College Station. 2011 May.

Aflatoxins are toxic organic compounds produced by fungi in grains. Moderately contaminated grains that cannot be used as food are often directed to animal feed. Economically-feasible detoxification measures for contaminated feeds are needed. The objectives of this research were to identify effective bentonites as aflatoxin adsorbents and to evaluate the performance of the clays as aflatoxin amendments in feed for broiler chickens.

Five bentonite samples from Gonzales, Texas, USA were collected and analyzed against the published selection criteria for aflatoxin adsorbents (Dixon et al, 2008): aflatoxin adsorption capacity, pH, CEC, organic carbon, particle size distribution, and mineralogical and structural compositions. Two bentonites were identified as potentially good aflatoxin adsorbents based on the analyses. These two bentonites were selected for an in vivo poultry experiment where chickens were fed with aflatoxin-contaminated corn (1400 ppb) to test the detoxification efficacy of the clays. Detailed mineralogy analyses were conducted on these two samples (4TX and 1TX) after size fractionation. Clay 4TX and 1TX contained 87% and 65% clay, respectively. Smectite was the dominant mineral phase in both clay fractions. Quartz and feldspars were also present in both samples. These minerals are unlikely to cause harmful effects on the chickens. The presence of pyrite and heavy metals in 1TX raised concerns about its use in animal feed.

The clays were introduced into feed by mixing the dry bentonite powder with the feed for twelve minutes in a mechanical mixer. The body weight was increased by 21% with clay 4TX and 14% with clay 1TX in the aflatoxin diet. The concentration of total aflatoxins in liver was reduced by 36% with clays addition. Liver visual appearance was also improved from pale red to more reddish color resembling the healthy red livers. All chickens under clean feed had significantly higher body weights than those fed with highly contaminated feed, suggesting that the clays did not completely eliminate the aflatoxins toxicity.

The published aflatoxin binder selection criteria were useful for screening bentonites as aflatoxins amendment. The selected bentonites based on the criteria could effectively sequester aflatoxins in vivo. Yet direct mixing bentonite as dry powder to highly contaminated poultry feed could not eliminate the toxicity of aflatoxins.

4 Journal Pulbications

1. Deng, Y. and M. Szczerba. 2011 Computational evaluation of bonding between aflatoxin B_1 and smectite. *Applied Clay Science.* 54(2011) 26–33. (see appendices)

2. Barrientos-Velázquez, A.L., R. Kakani, J. Fowler, A. Haq, C.A. Bailey, J.B. Dixon, and Y. Deng. Aflatoxin adsorption by bentonites in poultry feed. (in revision) (see appendices)

5 Appendices

Applied Clay Science 54 (2011) 26–33

Contents lists available at ScienceDirect

Applied Clay Science

journal homepage: www.elsevier.com/locate/clay

Research Paper

Computational evaluation of bonding between aflatoxin B_1 and smectite

Youjun Deng [a,*], Marek Szczerba [b]

[a] Department of Soil and Crop Sciences, Texas A&M University College Station, TX 77843-2474, United States
[b] Institute of Geological Sciences, Polish Academy of Sciences, Kraków Research Centre, ul. Senacka 1, 31-002 Kraków, Poland

ARTICLE INFO

Article history:
Received 19 January 2011
Received in revised form 10 June 2011
Accepted 9 July 2011
Available online 15 August 2011

Keywords:
Aflatoxin B1
Smectite
Bonding
Simulation

ABSTRACT

Certain smectites can effectively adsorb aflatoxin B_1 but the interaction between the toxin and smectites is still poorly understood. The objective of this study was to computationally evaluate the bonding mechanism between aflatoxin B_1 and smectite. Geometry optimization, net atomic charge distribution, vibration frequency and vibration intensity computations were performed for aflatoxin B_1 and cation–aflatoxin B_1 complexes. Molecular dynamics simulation was conducted for moist and dehydrated aflatoxin B_1–Na–smectite complexes. The computed energies, net atomic charge distribution, and molecular dynamics simulations consistently revealed that the two carbonyl oxygen were the most important interacting sites with exchange cations and H_2O in smectite interlayer. The two dihydrofuran oxygen had much less contribution to the bonding. Substantial charge redistribution and bond length changes occurred when cation–aflatoxin B_1 complexes formed. The computed vibration frequency shifts and vibration intensity changes were in excellent agreement with experimental observations reported in the literature. The calculations confirmed the importance of carbonyl groups in the bonding of aflatoxin to smectite and revealed more subtle interactions between exchange cations and the dihydrofuran oxygen.

1. Introduction

Aflatoxin B_1 (AfB_1) is a carcinogenic mycotoxin (Grant and Phillips, 1998) and can cause severe health problems and even death in animals and humans. Using smectite-rich clays, particularly Ca-bentonites, to alleviate the toxicity of aflatoxins has been tested for more than 30 years by animal scientists and toxicologists in many countries (e.g., Afriyie-Gyawu et al., 2008a,b; Chaturvedi et al., 2002; Chaturvedi and Singh, 2002; Desheng et al., 2005; Magnoli et al., 2008a,b; Márquez and Hernandez, 1995; Masimango et al., 1978, 1979; Nahm, 1995; Phillips et al., 1988, 2008; Wang et al., 2008). The effectiveness of the clays has been demonstrated by these animal feed experiments and human clinical trials.

To understand the interaction between the toxins and the clays so that other reactive clays can be selected or the less effective clays can be improved, several groups explored the thermodynamics of the adsorption, mineralogical criteria, and bonding mechanism between AfB_1 and smectites (Deng et al., 2010; Dixon et al., 2008; Kannewischer et al., 2006; Mulder et al., 2008; Tenorio et al., 2008). Deng et al. (2010) observed that AfB_1 could occupy the interlayer space of smectites. They further suggested that the major bonding mechanisms were ion–dipole interactions/coordination between the two carbonyl groups and the exchange cations when the smectite was dry, and H-bonding between the carbonyl groups with H_2O in the hydration shell of the exchange cations when the smectite was wet. There were several other proposed bonding models, such as electron donor–acceptor model (Phillips, 1999; Phillips et al., 2006, 2008), chelating of the two carbonyl groups with uncoordinated edge aluminum (Phillips et al., 1994), hydrogen bonding on smectite edge (Desheng et al., 2005), and bonding with the epoxidized C10=C11 (Fig. 1) (Tenorio et al., 2008). Which bonding mechanism is the dominating one in the adsorption of aflatoxin by smectite?

When smectites adsorb simple O-containing organic compounds such as aldehydes, ketones, alcohols, ethers, amides, and carboxylic acids, it is the oxygen atoms that play the most critical roles in the bonding through ion–dipole interaction or H-bonding (Theng, 1974). There are six oxygen atoms in an AfB_1 molecule (Fig. 1), the importance of carbonyl oxygen of AfB1 in the bonding was realized by several researchers (e.g., Deng et al., 2010; Phillips et al., 1994), but the role of other non-carbonyl oxygen at positions 9, 12, 13, and 17 in AfB_1 is still not clear. There are several possible positions for the exchange cation to interact with the oxygen individually or simultaneously as shown in Fig. 1. The objectives of this study were (1) to computationally evaluate the adsorption models of AfB_1–smectite complexes and (2) to refine the bonding mechanism between AfB_1 and smectite.

2. Molecular simulations

2.1. Molecular geometry and vibrational bands

Molecular geometry optimization of AfB_1 molecules were performed with Density Functional Theory (DFT) at the PCM/B3LYP/DGDZVP level

* Corresponding author. Tel.: +1 979 862 8476; fax: +1 979 845 0456.
E-mail addresses: yjd@tamu.edu (Y. Deng), ndszczer@cyf-kr.edu.pl (M. Szczerba).

0169-1317/$ – see front matter © 2011 Elsevier B.V. All rights reserved.
doi:10.1016/j.clay.2011.07.007

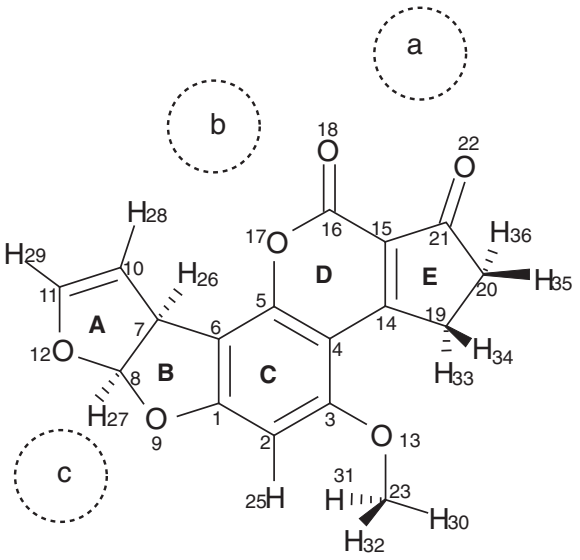

Fig. 1. Likely positions (a, b, and c) for exchange cations to interact with an AfB_1 in smectite.

of theory (Becke, 1993; Lee et al., 1988; Miertus et al., 1981) using Gaussian Inc. software (Frisch et al., 2004). After AfB_1 and the proposed cation–AfB_1 complex structures were optimized, the distribution of Mulliken atomic charge, vibration frequencies, and vibration intensities were computed. Vibration modes were visualized with software ChemCraft. The surface electrostatic potential map of AfB_1 was created with software VEGA ZZ (Pedretti et al., 2004). Potential Energy Distributions (PED) of vibrational bands were calculated with software GAR2PED (Martin and Van Alsenoy, 1995). The calculated frequencies, intensities, and PED of vibrational fundamentals of AfB_1 and of K-, Na-, Ca-, Mg-, and Mn–AfB_1 complexes were tabulated and are available from the authors upon request.

2.2. Molecular dynamics

Molecular dynamics of moist and dehydrated aflatoxin B_1–Na–smectite (AfB_1–Na–Sm) complexes at constant pressure and temperature (NPT) ensemble was simulated with program DLPOLY 2 (Smith and Forester, 1996). The simulation included two layers of smectite consisting of 64 unit cells (8a×4b×2c, 2560 structural atoms). A 0.5 octahedral charge per half unit cell was assumed for the smectite model [$Na_{0.5}(Al_{1.5}Mg_{0.5})Si_4O_{10}(OH)_2$]. Eleven aflatoxin B_1 molecules [$C_{17}H_{12}O_6$] and 32 Na^+ ions were included in each of the two interlayer spaces. The number of interlayer aflatoxin molecules was based on the maximum adsorption capacity (about 14% of smectite's mass) determined from the adsorption isotherm (Deng et al., 2010). To simulate the moist complex, a total of 255 water molecules (about 10% of smectite mass) were introduced into the two interlayer spaces. The charge and potential for H_2O were taken from the SPC-E model (Berendsen et al., 1987), for AfB_1 from the OPLS-AA force field (e.g., Jorgensen et al., 1996), and for smectite and exchange Na^+ from the CLAYFF force field (Cygan et al., 2004). Interactions among water molecules, AfB_1, and the mineral surface were calculated using standard Lorentz–Berthelot mixing rules (e.g., Cygan et al., 2004). A 50,000-step molecular dynamics simulation at 298 K was carried out for a 50-picosecond (ps) period with a time step of 0.001 ps. The last 10,000 time steps were used in the analysis of radial distribution functions.

The basal spacing from the molecular dynamics simulation was compared with that of AfB_1–Na–Sm complex synthesized by Deng et al. (2010). The basal spacing of the synthetic AfB_1–Na–Sm complex was measured with X-ray diffraction at 0% (nitrogen purge), 51% (room humidity), and 100% humidity in a reaction chamber at 30 °C described by Deng et al. (2010).

3. Results and discussion

3.1. Molecular configuration and energy

Our optimized aflatoxin B_1 configuration (Fig. 2 b) was nearly identical to those measured experimentally (van Soest and Peerdeman, 1970 a,b) and calculated theoretically (Billes et al., 2006). The molecule had a co-planar configuration of which the B, C, D, and E rings, two carbonyl groups, and the methoxy group lay in one plane. The dihydrofuran ring A protruded toward the viewer in Figs. 1 and 2. The methoxy group was repulsed from hydrogen atoms H33 and H34 of ring E.

Energy calculation after configuration optimization suggested that interactions of both Na^+ and Mn^{2+} with the two carbonyl oxygen at position *a* (Fig. 1) resulted in the lowest energy compared to the interactions at positions *b* and *c*. More than 96% of interactions between the exchange cations and AfB_1 would occur with the two carbonyl oxygen at position *a*, and only a small portion of the interactions might occur with the lactone ring oxygen (O17) and the dihydrofuran oxygen (Table 1).

3.2. Charge distribution and surface electrostatic potential of aflatoxin B_1

The two carbonyl oxygen had moderate negative charge but their surface electrostatic potential was the most negative (−0.22 atomic charge units, Fig. 2 b). Surface electrostatic potential at sites near the two dihydrofuran oxygen was less negative (about −0.1 atomic charge units). The most positive surface electrostatic potential was on the

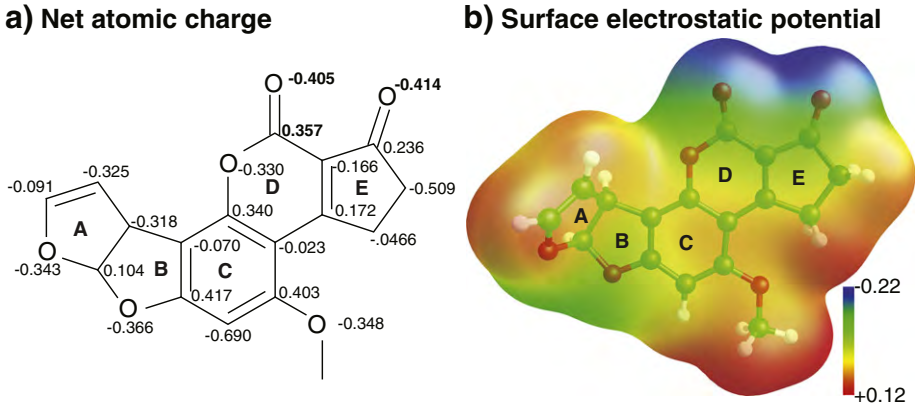

Fig. 2. Net atomic charge (a) of non-hydrogen atoms and surface electrostatic potential (b) of AfB_1. Unit: elementary charge.

Table 1
Energy analysis of Na– and Mn–AfB_1 complexes coordinated at positions *a*, *b*, and *c* as shown in Fig. 1.

Cation	Position	PCM* energy (kcal/mol)		Portion (%) at equilibrium
		Absolute	Relative	
Na	a	−796,163.7	0.0	96.3
	b	−796,159.7	4.0	3.3
	c	−796,157.0	6.6	0.4
Mn	a	−1,416,390.9	0.0	99.8
	b	−1,416,383.2	7.7	0.2
	c	−1,416,369.3	21.6	0.0

*PCM: polarizable continuum model

methyl group (CH_3). The calculated surface electrostatic potential was consistent with the AfB_1 crystal structure determined by X-ray diffraction (van Soest and Peerdeman, 1970a, b): two AfB_1 molecules were linked together by H-bonds between the carbonyl oxygen of one molecule and the other's methyl group. The surface electrostatic distribution indicated that the two carbonyl oxygen should be the most important reaction sites when AfB_1 coordinated with the positively charged exchange cations in smectite. The two dihydrofuran oxygen (position c in Fig. 1) were the next possible reacting sites for the exchange cations.

3.3. Molecular dynamics simulation

Molecular dynamics simulation of dehydrated AfB_1–Na–Sm complex revealed that exchange Na^+ cations migrated to the basal surfaces of smectite whereas AfB_1 molecules remained in the centers of the interlayer spaces (Fig. 3, a1). The major plane of AfB_1 lay parallel to smectite basal surfaces. The dehydrated AfB_1–Na–Sm complex had a 1.33 nm basal spacing, which was close to the experimentally measured value of 1.28 nm from the synthetical AfB_1–Na–Sm complex at 0% humidity. The minor difference was likely due to incomplete saturation of AfB_1 in the synthesized complex. In the moist AfB_1–Na–Sm complex, the major plane of AfB_1 slightly tilted toward smectite basal surfaces (Fig. 3, b1). H_2O filled the space between Na^+ ions, AfB_1, and smectite surfaces. The simulated moist AfB_1–Na–Sm complex was expanded to 1.52 nm in basal spacing. Experimental measurements of the synthesized AfB_1–Na–Sm complex had a basal spacing of 1.3 nm at 51% humidity and of a more varied basal spacing of 1.4–1.6 nm at nearly 100% humidity. The assumed 10% (mass) moist content in the computation was probably equivalent to a humidity close to 100%.

The molecular dynamics simulation illustrated that the carbonyl oxygen closely approached the exchange Na^+ ions (the A_1 and A_2 types in Fig. 3, a2). Most AfB_1 molecules interacted with the exchange cations by docking one exchange cation into two carbonyl oxygen (the A_1 type), a few of them through individual interaction between one of the two carbonyl oxygen with one cation (the A_2 type). The molecular dynamics simulation also suggested that some dihydrofuran oxygen were in close proximity to the exchange cations (the C type). Interactions between Na^+ and other AfB_1 oxygen atoms (e.g., the B type) were of much less importance. In the moist AfB_1–Na–Sm complex (Fig. 3, b2), all the above bonding types were observed. Moreover, interactions between the AfB_1 oxygen and water molecules (H-bonding) were common. Many of the carbonyl oxygen and dihydrofuran oxygen were in direct contact with both water molecules and Na^+ ions. Each Na^+ ion was surrounded by different numbers of water molecules.

The radial distribution functions offered a more quantitative estimation of the bonding probability. In the dehydrated AfB_1–Na–Sm complex, the Na^+ ions were coordinated mainly to the carbonyl oxygen with a bond length of 2.3 Å (Fig. 4 a, solid line). Direct interactions between Na^+ ions and the dihydrofuran oxygen with an average bond length of 2.4 Å were also important (Fig. 4 a, dashed line). In the moist AfB_1–Na–Sm complex, the Na^+ ions were mainly bonded to water molecules (Fig. 4 b, dashed grey line), which suggested that cation hydration expelled AfB_1 molecules from Na^+ ions. The carbonyl oxygen, however, also had nearly the same probability as H_2O to coordinate to

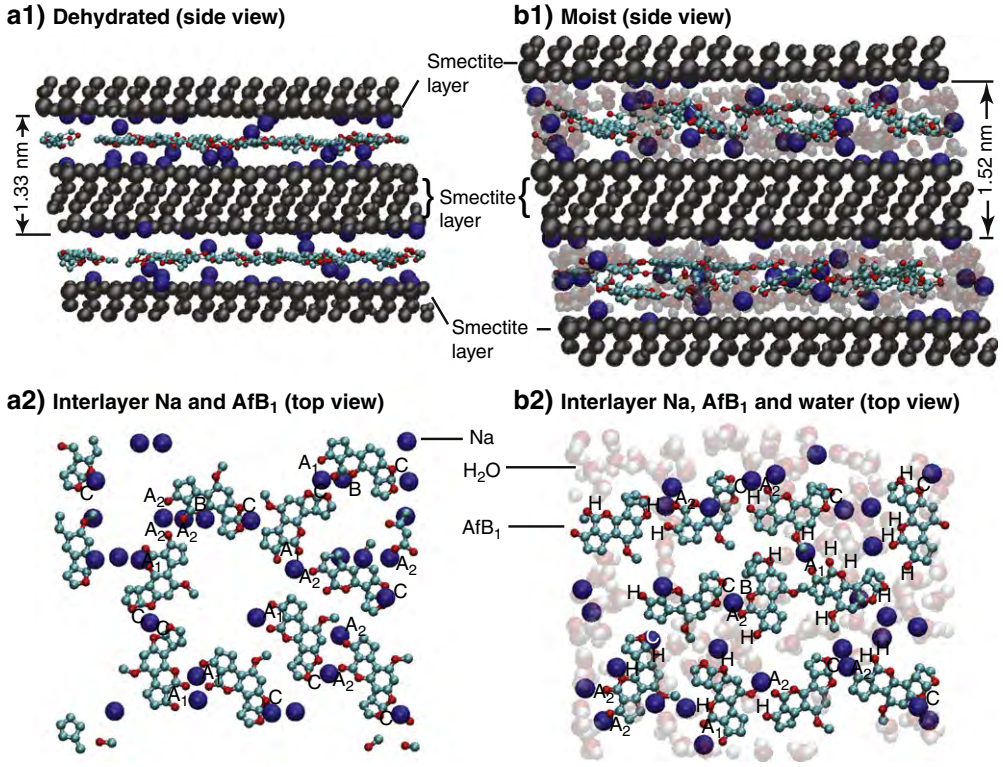

Fig. 3. Optimized structures from molecular dynamics simulation of dehydrated (a1 and a2) and moist (b1 and b2) AfB_1–Na–smectite complexes. Top images are side views of the complexes and bottom images are top views of the interlayer Na, AfB_1 and water molecules.

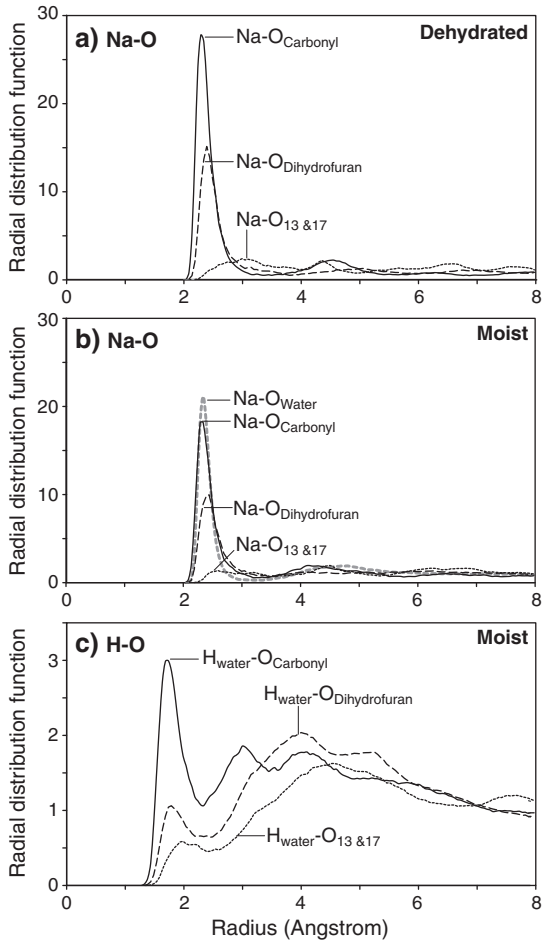

Fig. 4. Radial distribution functions of interlayer sodium ions (a and b) to oxygen atoms in AfB_1 and water molecules, and of water hydrogens (c) to AfB_1 oxygen based on the last 10,000 time step molecular dynamics simulations of the AfB_1–Na–smectite complexes.

Na^+ ions (Fig. 4b, solid line). In both dehydrated and moist AfB_1–Na–Sm complexes, the dihydrofuran oxygen had nearly 50% probabilities as carbonyl oxygen to bond to Na^+ ions. Interactions of Na^+ ions with other oxygen (O13 and O17) were negligible in both complexes (Fig. 4 a and b, dotted lines). The water hydrogen to AfB_1 oxygen radial distribution functions (Fig. 4c) suggested that the carbonyl oxygen also had higher probability than other oxygen to form H-bonds with H_2O in the moist AfB_1–Na–Sm complex.

The molecular dynamics revealed higher probabilities of cation–AfB_1 reaction at position *b* and *c* than the energy analysis did (Table 1). The discrepancy could be attributed to the different approaches used in the two computation methods and the different Na/AfB_1 ratios in the two approaches. Moreover, in the molecular dynamics, ions in smectite interlayer tended to reach relatively uniform distributions because of the repulsion between them and the bonding between ions and clays were stronger than between ions and AfB_1. As shown in Fig. 3, the exchange Na^+ cations are strongly attracted to the basal surfaces of the dehydrated smectite. We have tried to set the initial positions of the exchange cations in the middle of the interlayer space so that they would have more chances to form co-planar complexes with the aflatoxin as shown in Fig. 1, but the cations moved to the basal surfaces rapidly.

The molecular dynamics simulation suggested that the carbonyl groups would be the major functional groups in the coordination between exchange cations and AfB_1 molecules. The dihydrofuran oxygen also would contribute to the bonding with less importance. The presence of water molecules would compete with AfB_1 molecules for the exchange cations, but they would not be able to diminish the direct bonding between exchange cations and the AfB_1 molecules at the tested moisture content (about 10% by mass). Direct interactions between exchange cations and carbonyl oxygen suggested that bonding strength between smectite and AfB_1 should be affected by cation type in both dehydrated and moist AfB_1–Na–Sm complexes. Infrared bands of adsorbed AfB_1 should shift when Na was replaced by other cations. The predicted shifts were indeed observed in AfB_1–Sm saturated with Ca, Mg, La, Al, Cu, Mn, and Ni cations in the experiment of Deng et al. (2010).

3.4. Charge redistribution and configuration changes of AfB_1 after interacting with different exchange cations

Our calculation revealed that, after interacting with the AfB_1 carbonyl groups via ion–dipole interaction or coordination, exchange cations possessed less positive charge than their ideal valences. This meant that electrons shifted from AfB_1 toward the exchange cations. Bonding between exchange cation and carbonyl oxygen led to substantial charge redistribution on atoms in AfB_1: atoms that were directly involved in the bonding i.e., O18 and O22, and their immediate neighboring C16 and C21 had the greatest charge changes with a magnitude of 0.1–0.2 atomic charge units (Fig. 5). The carbonyl oxygen became more negative and the carbons became more positive. The magnitudes of these changes increased when the ion–dipole interaction/coordination was enhanced by increasing cation valence, reducing ion radius, or introducing a transition heavy metal cation. The net charge changes suggested electron shift from C16 and C21 to O18, O22 and C15.

The basic co-planar AfB_1 molecular configuration was well preserved in the ion–dipole interaction or coordination. The cations fell in the same plane. The carbonyl group-cation distance decreased when cation valence/radius ratio increased: a nearly 0.8 Å reduction was observed when the cation was changed from K^+ to Mg^{2+}, which suggested an enhanced ion–dipole interaction. Transition metal Mn^{2+} was slightly more distant from the carbonyl groups than Mg^{2+}. With increasing cation charge/radius ratio, the neighboring bonds shrank and expanded alternatively (Fig. 6): the greatest elongations occurred on the two carbonyl groups (C16O18 and C21O22), and the greatest shrinkage occurred on their immediately adjacent bonds O17C16, C21C15, and C16C15. The

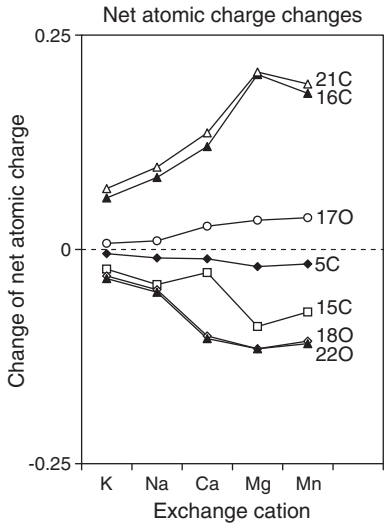

Fig. 5. Net atomic charge changes in AfB_1 molecules coordinated to different exchange cations through the two carbonyl oxygen. Other atoms had fewer changes in net charge than the atoms shown in the figure.

alternative elongation/shrinkage propagated to rings C, B, and A with reducing amplitudes.

3.5. Computed vibrational band positions and intensities

When exchange cations interacted with AfB_1 at position *a* as shown in Fig. 1, several AfB_1 infrared band positions shifted and band intensity changed substantially compared to a free aflatoxin molecule. The greatest changes were observed on the carbonyl bonds and their adjacent bonds. Both in-phase and opposite-phase stretching vibrations of the two carbonyl bonds (Fig. 7A and B) shifted to lower frequencies (Fig. 8A and B). When AfB_1 was bonded to Mn^{2+}, a 60 cm^{-1} red shift was observed on the in-phase stretching vibration (Fig. 8A) and a 112 cm^{-1} red shift was observed on the opposite-phase stretching vibrations (Fig. 8B). These shifts suggested substantial weakening of the carbonyl bonds after coordinating to Mn^{2+}. The calculation also indicated that band intensities of opposite-phase stretching vibrations (Fig. 8B) of the two carbonyl groups were much weaker than their nearby bands, which may hinder the experimental observation of the shifts. Smaller red shifts (<13 cm^{-1}) were observed on vibrations that had less contribution from stretching vibrations of the carbonyl bonds (Figs. 7C, D, 8C, and D).

Several bands that contained the bending vibrations of the carbonyl bonds had blue shifts (Fig. 7E–I). The greatest blue shift was observed on the in-plane, symmetric swing vibrations of the two carbonyl groups (Fig. 7G). Interacting with Mg^{2+} resulted in the greatest blue shift of 67 cm^{-1} (Fig. 9G). Vibrations E, F, H, and I in Fig. 7 were mainly due to deformation of ring C, D, or E but much less from bending vibrations of the carbonyl bonds. These bands shifted less compared to band G.

In addition to band shifts, the potential energy distribution of the vibrations also changed with different cations. For example, the infrared band A (Fig. 8A) was mainly due to the in-phase carbonyl stretching vibrations when the cations were monovalent K or Na. When the cations were replaced with divalent Ca, Mg, or Mn, the deformational in-plane-bending vibrations of rings D and E contributed more to this vibration.

There were no significant changes in the computed band positions or band intensities in the 3000–3300 cm^{-1} range in which various C–H stretching vibrations occurred. Most bands in the range 450–800 cm^{-1} did not show more than 10 cm^{-1} shifts. When AfB_1 reacted with the cations, significant but not systematic changes in potential energy distributions were observed on the <450 cm^{-1} bands.

3.6. Comparison between computed and experimental infrared bands

Like most vibration frequency computation, the computed frequencies were higher than the experimental observations. Yet, the directions and magnitudes of calculated AfB_1 infrared band shifts were consistent with experimental observations reported by Deng et al. (2010): At nearly 0% humidity, the in-phase stretching vibrations of the two carbonyl bonds (Fig. 7A) in the AfB_1–smectite complexes red shifted in increasing magnitudes in the order of K<Na<Ca<Mg<Mn. The experimentally recorded frequency (1705 cm^{-1}) of the AfB_1–Mn–Sm was 31 cm^{-1} lower than that of the AfB_1–K–Sm. Only a shoulder at 1657 cm^{-1} was observed on the infrared spectrum of AfB_1–K–Sm, and this shoulder was attributed to the opposite-phase vibrations of the carbonyl groups (Fig. 7B). It was believed that this band was fused to the more intense bands at 1630 cm^{-1} in other cation saturated AfB_1–Sm complexes (Deng et al., 2010). This assignment agreed with the computed weak intensity of the opposite-phase stretching vibrations of carbonyl groups (Fig. 8B). It could be shaded by other nearby strong bands at about 1654 $cm^{-1}$and 1614 cm^{-1}, which were mainly due to the in-plane deformations of ring C (Fig. 8). The experimentally observed strong band at 1630 cm^{-1} must be corresponding to the computed 1654 cm^{-1} band in Fig. 8 due to the same characteristics in intensity and inertness to cation exchange. Small red shifts were observed on the poorly-resolved band at 1590 cm^{-1} on the experimental infrared spectra, this band must be corresponding to the computed 1616 cm^{-1} band (Fig. 8C).

The following shifts were observed on experimental spectra of K-, Na-, Ca-, Mg-, and Mn-saturated AfB_1–Sm complexes when the ion–dipole interaction/coordination was enhanced (Deng et al., 2010): (1) a 12 cm^{-1} red shift from 1550 cm^{-1} to 1538 cm^{-1} that must be corresponding to the computed D bands (Fig. 8D), (2) a 16 cm^{-1} blue shift from 1496 cm^{-1} to 1512 cm^{-1} that must be corresponding to the computed E bands (Fig. 8E), (3) a minor blue shift of the 1444 cm^{-1} band that must be corresponding to the computed F bands. The C–H stretching bands (2800–3300 cm^{-1}) and bands at 1208, 1246, 1273, 1304, and 1343 cm^{-1} did not show distinct shifts after cation exchange. This was in agreement with the computation.

3.7. Implication for selecting and modifying smectites to scavenge aflatoxins

The excellent agreement between computational results and the experimental observations suggested the importance of ion–dipole interactions in the bonding of aflatoxin to smectites. We speculate that the enhanced ion–dipole interaction of divalent cations with aflatoxin would increase the affinity of the smectite for the aflatoxin. Our preliminary results indicated that a more than 10 times of increase in the *k* constants of the Langmuir adsorption isotherms can be achieved by replacing exchange Na with Ca. The *k* constant reflects

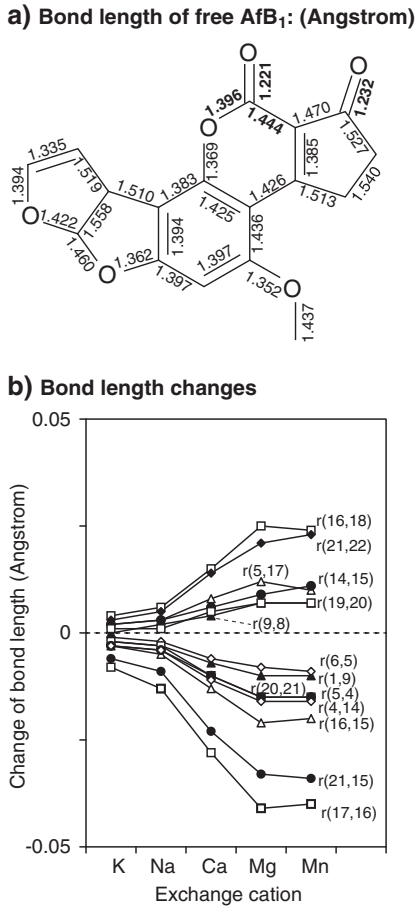

Fig. 6. Bond lengths of free AfB_1 (a) and their changes in AfB_1 molecules coordinated to different exchange cations through the two carbonyl oxygen (b). Other bonds had fewer changes than the bonds shown in the figure.

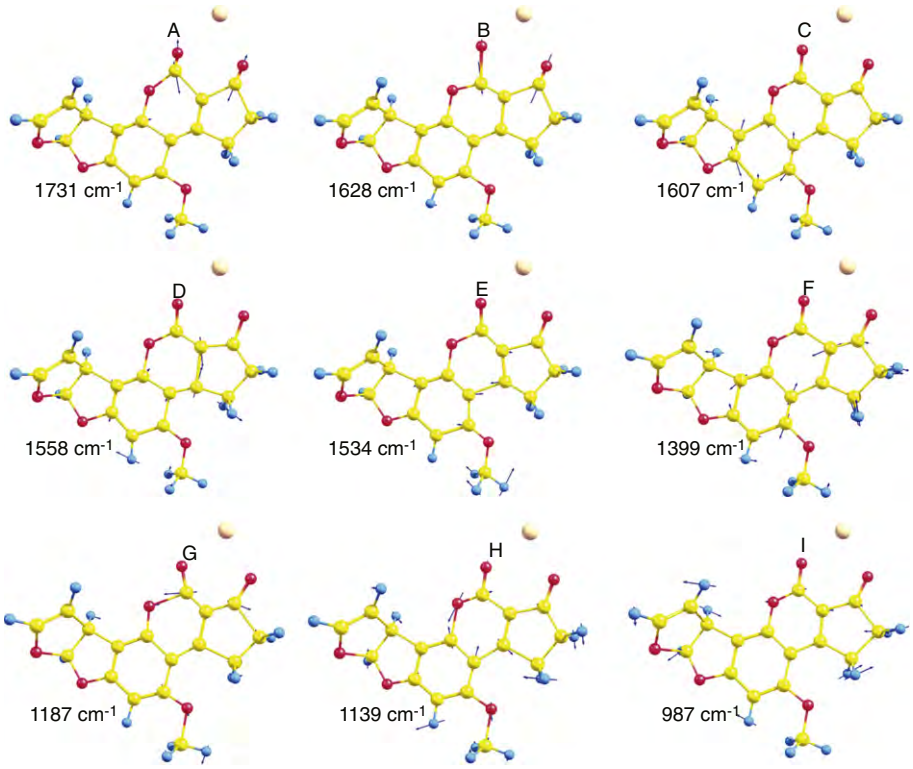

Fig. 7. Example Ca–AfB_1 molecular vibrations and their corresponding frequencies. The arrow axes represent the vibration directions and arrow lengths represent the vibration amplitudes.

the affinity of the mineral for aflatoxin. We further speculate that the size of nanometer scale domains between the exchanges cations in the interlayes, which can be varied by changing the cations or by changing the charge density of the smectite, would play a critical role in determining the selectivity of the smectite. We expect that high selectivity can be achieved when the size of the surface domain matches the size of an aflatoxin molecule. These speculations will be tested in our ongoing studies on the effects of smectite charge density and exchange cation types on the minerals' selectivity and adsorption capacity for aflatoxins.

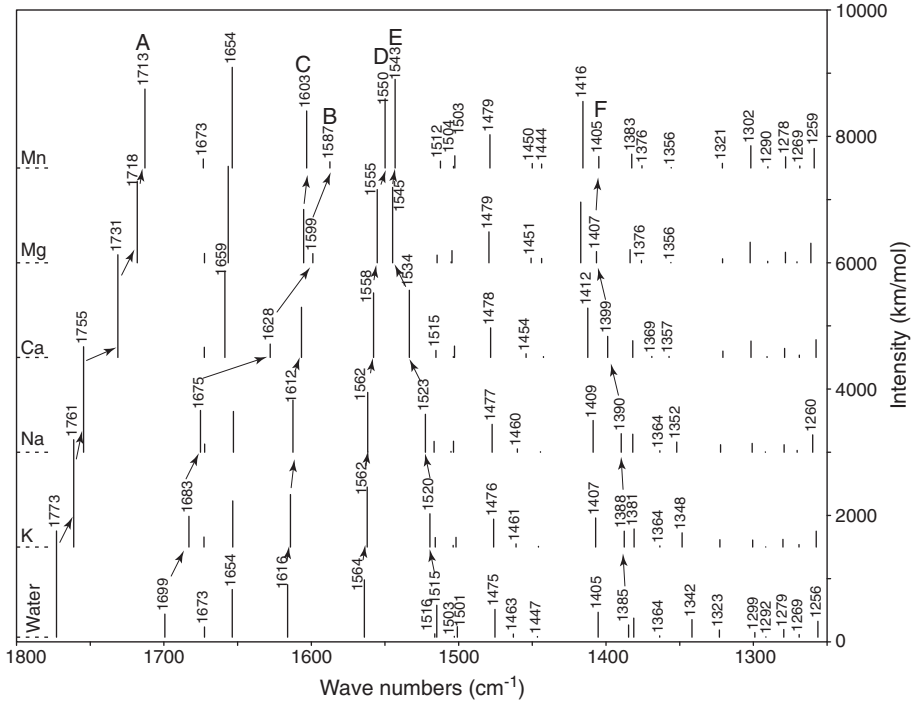

Fig. 8. Calculated 1250–1800 cm^{-1} infrared bands of AfB_1 and cation–AfB_1 complexes via cation–carbonyl oxygen coordination.

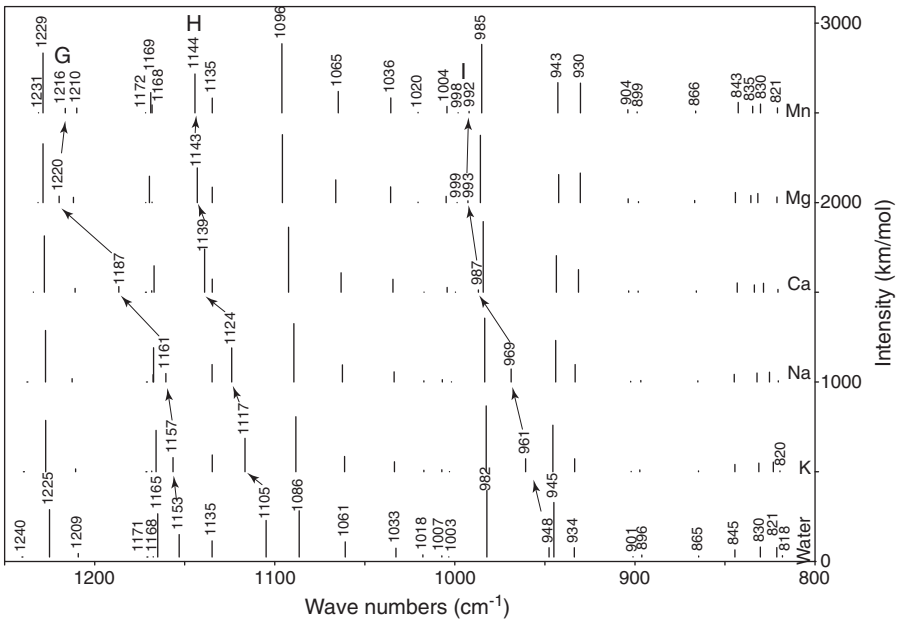

Fig. 9. Calculated 800–1250 cm^{-1} infrared bands of AfB_1 and cation–AfB_1 complexes via cation–carbonyl oxygen coordination.

4. Conclusions

Molecular geometry optimization, energy minimization, surface electrostatic potential calculation, and molecular dynamics simulation consistently suggested that the carbonyl oxygen on AfB_1 played the most important role in bonding of the toxin to smectite through ion–dipole interaction/coordination under fully and partially dehydrated conditions. The computed infrared band shifts and intensity changes of such bonding with different cations (K, Na, Ca, Mg, and Mn) were in excellent agreement with the reported infrared spectra recorded at near 0% humidity. The computations further indicated the bonding was mainly between the two carbonyl oxygen and exchange cations in the interlayer of smectite. The dihydrofuran oxygen might be involved in the bonding between AfB_1 and the exchange cations in smectite, but this interaction contributed less to the bonding. This improved understanding about the bonding mechanism offered important guidance for future smectite selection and modification to achieve high selectivity and high adsorption capacity in binding AfB_1.

Acknowledgements

Funding was partially supplied by the Texas AgrilLife Research, Texas Corn Producers Board, and National Corn Growers Association (USA).

Reference

Afriyie-Gyawu, E., Ankrah, N.A., Huebner, H.J., Ofosuhene, M., Kumi, J., Johnson, N.M., Tang, L., Xu, L., Jolly, P.E., Ellis, W.O., Ofori-Adjei, D., Williams, J.H., Wang, J.S., Phillips, T.D., 2008a. NovaSil clay intervention in Ghanaians at high risk for aflatoxicosis. I. Study design and clinical outcomes. Food Addit. Contam. Part A-Chem. 25 (1), 76–87.

Afriyie-Gyawu, E., Wang, Z., Ankrah, N.A., Xu, L., Johnson, N.M., Tang, L., Guan, H., Huebner, H.J., Jolly, P.E., Ellis, W.O., Taylor, R., Brattin, B., Ofori-Adjei, D., Williams, J.H., Wang, J.S., Phillips, T.D., 2008b. NovaSil clay does not affect the concentrations of vitamins A and E and nutrient minerals in serum samples from Ghanaians at high risk for aflatoxicosis. Food Addit. Contam. Part A-Chem. 25 (7), 872–884.

Becke, A.D., 1993. Density-functional thermochemistry. III. The role of exact exchange. J. Chem. Phys. 98 (7) 5648-3652.

Berendsen, H.J.C., Grigera, J.R., Straatsma, T.P., 1987. The missing term in effective pair potentials. J. Phys. Chem. 91 (24), 6269–6271.

Billes, F., Móricz, A.M., Tyihák, E., Mikosch, H., 2006. Simulated vibrational spectra of aflatoxins and their demethylated products and the estimation of the energies of the demethylation reactions. Spectrochim. Acta A 64 (3), 600–622.

Chaturvedi, V.B., Singh, K.S., 2002. Detoxification of aflatoxin by adsorbents. Indian J. Anim. Sci. 72 (10), 924–927.

Chaturvedi, V.B., Singh, K.S., Agnihotri, A.K., 2002. In vitro aflatoxin adsorption capacity of some indigenous aflatoxin adsorbents. Indian J. Anim. Sci. 72 (3), 257–260.

Cygan, R.T., Liang, J.-J., Kalinichev, A.G., 2004. Molecular models of hydroxide, oxyhydroxide, and clay phases and the development of a general force field. J. Phys. Chem. B 108 (4), 1255–1266.

Deng, Y., Barrientos Velazquez, A.L., Billes, F., Dixon, J.B., 2010. Bonding mechanisms between aflatoxin B_1 and smectite. Appl. Clay Sci. 50 (1), 92–98.

Desheng, Q., Fan, L., Yanhu, Y., Niya, Z., 2005. Adsorption of aflatoxin B-1 on montmorillonite. Poult. Sci. 84 (6), 959–961.

Dixon, J.B., Kannewischer, I., Tenorio Arvide, M.G., Barrientos Velazquez, A.L., 2008. Aflatoxin sequestration in animal feeds by quality-labeled smectite clays: an introductory plan. Appl. Clay Sci. 40, 201–208.

Frisch, M., Trucks, G., Schlegel, H., Scuseria, G., Robb, M., Cheeseman, J., Montgomery, J., Vreven, J., Kudin, K., Burant, J., Millam, J., Iyengar, S., Tomasi, J., Barone, V., Mannucci, B., Cossi, M., Scalmani, G., Rega, N., Petersson, G., Nakatsuji, H., Hada, M., Ehara, M., Toyota, K., Fukuda, F., Hasegawa, J., Ishida, M., Nakajima, T., Honda, Y., Kitao, O., Nakai, H., Klene, M., Li, X., Knox, J., Hratchian, H., Cross, J., Bakken, V., Adamo, C., Jramillo, J., Gomperts, R., Stratmann, R., Yazyev, O., Austin, A., Cammi, R., Pomelli, C., Ochterski, J., Ayala, P., Morokuma, K., Voth, G., Salvador, P., Dannenberg, J., Zakrzewski, V., Dapprich, S., Daniels, A., Strain, M., Frakas, O., Malick, D., Rabuck, A., Raghavachari, K., Foresman, J., Ortiz, J., Cui, Q., Baboul, A., Clifford, S., Cislowski, J., Stefanov, B., Liu, G., Liashenko, A., Piskorz, P., Komaromi, I., Martin, R., Fox, D., Keith, T., Al-Laham, M., Peng, C., Nanayakkara, A., Challacombe, M., Gill, P., Johnson, B., Chen, W., Wong, M., Gonzalez, C., Pople, J., 2004. Gaussian-94, Revision, C.3. Gaussian, Inc, Pittsburgh, PA.

Grant, P.G., Phillips, T.D., 1998. Isothermal adsorption of aflatoxin B_1 on HSCAS clay. J. Agric. Food Chem. 46 (2), 599–605.

Jorgensen, W.L., Maxwell, D.S., Tirado-Rives, J., 1996. Development and testing of the OPLS all-atom force field on conformational energetics and properties of organic liquids. J. Am. Chem. Soc. 118 (45), 11225–11236.

Kannewischer, I., Tenorio, A.M.G., White, G.N., Dixon, J.B., 2006. Smectite clays as adsorbents of aflatoxin B1: initial steps. Clay Sci. 12 (Supplement 2), 199–204.

Lee, C., Yang, W., Parr, R.G., 1988. Development of the Colle–Salvetti correlation-energy formula into a functional of the electron density. Phys. Rev. B: Condens. Matter 37 (2), 759–785.

Magnoli, A.P., Cabaglieri, L.R., Magnoli, C.E., Monge, J.C., Miazzo, R.D., Peralta, M.F., Salvano, M.A., Rosa, C.A.R., Dalcero, A.M., Chiacchiera, S.M., 2008a. Bentonite performance on broiler chickens fed with diets containing natural levels of aflatoxin B_1. Rev. Bras. Med. Vet 30 (1), 55–60.

Magnoli, A.P., Tallone, L., Rosa, C.A.R., Dalcero, A.M., Chiacchiera, S.M., Torres Sanchez, R.M., 2008b. Commercial bentonites as detoxifier of broiler feed contaminated with aflatoxin. Appl. Clay Sci. 40 (1–4), 63–71.

Márquez, R.N., Hernandez, I.T.D., 1995. Aflatoxin adsorbent capacity of two Mexican aluminosilicates in experimentally contaminated chick diets. Food Addit. Contam. 1995, 431–433.

Martin, J.M.L., Van Alsenoy, C., 1995. GAR2PED. University of Antwerp.

Masimango, N., Remacle, J., Ramaut, J., 1979. Elimination of aflatoxin B_1 from contaminated media by swollen clays. Ann. Nutr. Aliment. 33 (1) 137–1–47.

Masimango, N., Remacle, J., Ramaut, J.L., 1978. The role of adsorption in the elimination of aflatoxin B_1 from contaminated media. Eur. J. Appl. Microbiol. Biotechnol. 6 (1), 101–105.

Miertus, S., Scrocco, E., Tomasi, J., 1981. Electrostatic interaction of a solute with a continuum. A direct utilization of ab initio molecular potentials for the prevision of solvent effects. Chem. Phys. 55 (1), 117–129.
Mulder, I., Tenorio Arvide, M.G., White, G.N., Dixon, J.B., 2008. Smectite clay sequestration of aflatoxin B1: mineral dispersivity and morphology. Clays Clay Miner. 56, 559–571.
Nahm, K.H., 1995. Prevention of aflatoxicosis by addition of antioxidants and hydrated sodium calcium aluminosilicate to the diet of young chicks. Nippon Kakin Gakkaishi 32 (2), 117–127.
Pedretti, A., Villa, L., Vistoli, G., 2004. VEGA — An open platform to develop chemo-bio-informatics applications, using plug-in architecture and script programming. J. Comput. Aided Mol. Des. 18 (3), 167–173.
Phillips, T.D., 1999. Dietary clay in the chemoprevention of aflatoxin-induced disease. Toxicol. Sci. 52 (2), 118–126.
Phillips, T.D., Afriyie-Gyawu, E., Wang, J.S., Williams, J.O., Huebner, H., 2006. The potential of aflatoxin sequestering clay. In: Barug, D., Bhatnagar, D., van Egmond, H.P., van Der Kamp, J.W., van Osenbruggen, W.A., Visconti, A. (Eds.), The Mycotoxin Factbook: Food and Feed Topics. Wageningen Academic Publishers, Wageningen, The Netherlands, pp. 329–346.
Phillips, T.D., Afriyie-Gyawu, E., Williams, J., Huebner, H., Ankrah, N.A., Ofori-Adjei, D., Jolly, P., Johnson, N., Taylor, J., Marroquin-Cardona, A., Xu, L., Tang, L., Wang, J.S., 2008. Reducing human exposure to aflatoxin through the use of clay: a review. Food Addit. Contam. Part A-Chem. 25 (2), 134–145.
Phillips, T.D., Clement, B.A., Park, D.L., 1994. Approaches to reduction of aflatoxins in foods and feeds. In: Eaton, D.L., Groopman, J.D. (Eds.), The Toxicology of Aflatoxins: Human Health, Veterinary, and Agricultural Significance. Academic Press, San Diego, pp. 383–406.
Phillips, T.D., Kubena, L.F., Harvey, R.B., Taylor, D.R., Heidelbaugh, N.D., 1988. Hydrated sodium calcium aluminosilicate: a high affinity sorbent for aflatoxin. Poult. Sci. 67, 243–247.
Smith, W., Forester, T.R., 1996. DL-POLY _2.0: a general-purpose parallel molecular dynamics simulation package. J. Mol. Graphics 14 (3), 136–141.
Tenorio, A.M.G., Mulder, I., Dixon, J.B., 2008. Smectite clay adsorption of aflatoxin vs. octahedral composition as indicated by FTIR. Clays Clay Miner. 56 (5), 571–578.
Theng, B.K.G., 1974. The Chemistry of Clay-Organic Reactions. John Wiley and Sons, New York.
van Soest, T.C., Peerdeman, A.F., 1970a. The crystal structures of aflatoxin B_1. I. The structure of the chloroform solvate of aflatoxin B_1 and the absolute configuration of aflatoxin B_1. Acta Cryst B26, 1940–1947.
van Soest, T.C., Peerdeman, A.F., 1970b. The crystal structures of aflatoxin B_1. II. The structure of an orthorhombic and a monoclinic modification. Acta Cryst B26, 1947–1955.
Wang, P., Afriyie-Gyawu, E., Tang, Y., Johnson, N.M., Xu, L., Tang, L., Huebner, H.J., Ankrah, N.A., Ofori-Adjei, D., Ellis, W., Jolly, P.E., Williams, J.H., Wang, J.S., Phillips, T.D., 2008. NovaSil clay intervention in Ghanaians at high risk for aflatoxicosis: II. Reduction in biomarkers of aflatoxin exposure in blood and urine. Food Addit. Contam. Part A-Chem. 25 (5), 622–634.

Aflatoxin adsorption by bentonites in poultry feed

A.L. Barrientos-Velázquez[1], R. Kakani[2], J. Fowler[2], A. Haq[2], C.A. Bailey[2], J.B. Dixon[1], Y. Deng[1]

[1]Soil & Crop Sciences Department, [2]Poultry Science Department, Texas A& M University

Abstract

Aflatoxins are produced by fungi Aspergillus flavus and parasiticus that contaminates a variety of grains. Aflatoxins are highly toxic and had been related to liver cancer in animals an humans. Several animal experiments had shown consistently reduction of aflatoxin bioavailability to animals by including montmorillonite in the diet. Yet, a large variation in the in vivo protection capacity among samples had been observed. Several authors had related smectite properties to in vitro aflatoxin adsorption. The objectives of this reseach were 1) to compare physical, chemical and mineralogical properties of bentonites and relate them with their adsorption efficacy, 2)to evaluate the efficacy of selected clays as amendments of aflatoxin contaminated feed of broiler chickens, and 3) to address the safety of the clays when incorporated in the diet. Two bentonites from Texas were identified as potentially good aflatoxin adsorbents based on in vitro analyses. Detailed mineralogy analyses were conducted on these two samples (4TX and 1TX) after size fractionation. Clay 4TX and 1TX contained 87% and 65% clay, respectively. Smectite was the dominant mineral phase in both clay fractions. Quartz and feldspars were also present in both samples. These minerals are unlikely to cause harmful effects on the chickens. The presence of pyrite and heavy metals in 1TX raised concerns about its use in animal feed. The clays were introduced into feed by mixing the dry bentonite powder with the feed for twelve minutes in a mechanical mixer. The body weight was increased by 21% with clay 4TX and 14% with clay 1TX in the aflatoxin diet. The concentration of total aflatoxins in liver was reduced by 36% with the addition of clays. Liver visual appearance was also improved from pale red to a more reddish color resembling the healthy red liver. All chickens fed clean feed had significantly higher body weights than those fed with highly contaminated feed, suggesting that the clays did not completely eliminate aflatoxin toxicity. The published aflatoxin binder selection criteria were useful for screening bentonites as aflatoxin amendments. The selected bentonites based on the criteria could effectively sequester aflatoxins in vivo. Yet direct mixing of bentonite as dry powder to highly contaminated poultry feed could not eliminate the toxicity of aflatoxins.

1 Introduction

Grain that contains 20 to 300 ppb aflatoxins cannot be used in food but can be directed to feed with certain limitations made by the Food and Drug Administration (FDA). For young animals and dairy cows the aflatoxin concentration cannot exceed the same level as for human consumption (20 ppb). This is because younger animals are more susceptible to the effects of aflatoxins. Although the aflatoxin levels from 100 to 300 ppb may not cause acute toxicity to certain animals like ruminants, their performance can be compromised as indicated by a reduction in milk production (Jouany and Diaz, 2005).

There are many proposed methods to inactivate, degrade, or remove aflatoxin in food and feed (Phillips et al., 1994). Among the decontamination techniques, incorporation of adsorbents in the diet of animals exposed to aflatoxin

has been extensively investigated. Due to their low cost and wide availability, use of adsorbents is the one of the most economically feasible techniques that can be used to protect animals from the deleterious effects of aflatoxins.

A wide range of animals had been tested in evaluate the effectiveness of adsorbents for aflatoxins. Pigs (Lindemann et al., 1993; Thieu and Pettersson, 2008) and turkeys (Ramos and Hernandez, 1996) had shown improvement in body weight and reduce mortality by clay incorporation in the diet. Adding bentonite to feed also reduced the concentration of other less toxic residue forms of aflatoxin in milk in a dairy cows study (Stroud et al., 2006) and in goats (Ramos and Hernandez, 1996). The bentonite adsorbs aflatoxin in the gastrointestinal track before it can be assimilated and metabolized by the organism (Phillips et al., 1987).

Poultry are highly susceptible to aflatoxins and their susceptibility is only, after ducks and turkeys (Arafa et al., 1981; Dalvi, 1986; Leeson et al., 1995). Due to the economic significance and rapid growth, chickens are usually selected for animal trials to test exposure effects to different levels of aflatoxins or to evaluate the efficacy of aflatoxin binders. Addition of a hydrated sodium calcium alumino silicate (HSCAS) and bentonites in the aflatoxin diet of chicken had shown to significantly improve body weight (Phillips et al., 1988; Kubena et al., 1990; Rosa et al., 2001; Pimpukdee et al., 2004; Bailey et al., 2006; Phillips and Carpenter, 2008; Kermanshashi et al., 2009). The adsorption capacity of bentonites can be highly variable, which may result in different effectiveness in detoxifying aflatoxins in vivo. Detailed mineralogical and chemical characterization of these aflatoxin binders can help to understand the variation in adsorption effectiveness observed in animal experiments (Pasha et al., 2007) and therefore, to further narrow down the selections of screened binding candidates for animal feed experiments.

The objectives of this study were 1) to perform detailed charactertization of the mineral components in the samples, 2) to evaluate the efficacy of selected clays as amendments of aflatoxin contaminated feed of broiler chickens, and 3) to address the safety of the clays when incorporated in the diet.

2 Materials and Methods

2.1 Characterization of bentonites as aflatoxin adsorbents

2.1.1 X-ray diffraction analysis

The sand and silt fractions were ground to pass a 140 mesh sieve. Bulk sample, sand and silt XRD powder patterns were recorded from 4 to 70 degrees two-theta using a D8 BRUKER ADVANCE diffractometer with Cu Kα radiation, 30 rpm spin rate, and 0.017 step size. A 1-D position sensitive detector LynxEye was used during XRD analyses.

Each clay fraction was saturated with Mg^{2+} to facilitate the identification of phyllosilicates as their d-spacing can shift, depending on interlayer cations, swelling, and heat treatments. Approximately 60 mg of each clay sample was

obtained by taking suitable amounts. The samples were saturated with 0.5M $MgCl_2$. The detailed procedure is described in the Soil Mineralogy Lab Manual (Deng et al., 2009). The suspensions of Mg- or K-saturated clays were air dried on glass discs. The XRD patterns of magnesium saturated clays were recorded at room humidity and after glycerol solvation.

To confirm the aflatoxin intercalation into smectite, basal spacings of the clays before and after aflatoxin adsorption were measured by XRD at room humidity and 0 % humidity. Each clay suspension was air dried on a zero-background quartz slide and the slide was placed in an XRD 900 reactor chamber (Anton Paar). One XRD pattern was recorded at room humidity (40%) at 30°C, and a second pattern was recorded at nearly 0% humidity but the same temperature. The 0% humidity was achieved by alternative N_2 flushing and evacuating the chamber for 20 min. During XRD recording at 0% humidity, the chamber was filled with dry N_2.

2.1.2 Fourier transform infrared (FTIR) analysis

The spectra of the clay fractions were recorded using a Perkin Elmer Spectrum 100 with DRIFT accessory. The samples were diluted by mixing 0.01 g of sample with 0.3 g of KBr. Sixty-four scans from 4000 to 450 cm^{-1} at a resolution of 4 cm^{-1} were collected for each spectrum.

2.1.3 Aflatoxin adsorption isotherms

Aflatoxin adsorption isotherms were conducted on both unfractionated bulk samples and on the clay fraction of the samples. The adsorption capacities of the unfractionated samples were analyzed following the procedure described by Kannewischer et al., (2006). Diluted bentonite suspensions were prepared by dispersing 0.01 g of sample in 5 ml of distilled water. Fifty microliters of suspension, containing 0.1 mg bentonite, were transferred to a series 15 mL polypropylene centrifuge tubes. An 8-ppm aflatoxin solution was prepared by diluting a stock solution (1000 ppm AfB1 in acetronitrile), and then desired amounts of the 8-ppm aflatoxin solutions were added to the 15 mL to achieve the following aflatoxin concentrations: 0.0, 0.4, 1.6, 3.2, 4.8, 6.4, and 8.0 ppm. Each isotherm was duplicated. After overnight shaking at 200 motions per minute, the samples were centrifuged at 4500 rpm (5443.2 g) for 57 min. The aflatoxin concentration left in solution was analyzed using a Beckman Coulter DU 800 UV-spectrophotometer. The maximum adsorption was calculated using Langmuir isotherms.

The clay fractions (<2 μm) were also analyzed for adsorption capacity following a slightly modified procedure. The mass of the clay and volumes of the solutions were increased 10 times so there was enough clay (1mg) for XRD and FTIR analyses after the aflatoxin adsorption experiment. Clay suspension was prepared by diluting the dialyzed clay suspension to reach a final clay content of 1 mg per 5 mL. Five mL of the diluted clay suspension were added to 50 mL polypropylene centrifuge tubes. After the aflatoxin adsorption using only

two concentrations per sample, the clays were washed four times with distilled water. The supernatant after each washing was recovered and analyzed for aflatoxin concentration in order to measure desorption, and the clays were used for XRD and FTIR analyses.

2.2 In vivo poultry experiment

2.2.1 Feed preparation

Two sources of aflatoxin contaminated corn were used to achieve the desired aflatoxin level in the final poultry feed. One corn contained 803 ppb aflatoxin was provided by Dr. Tom Isakeit. The other corn was inoculated with Aspergillus parasiticus cultures (from Dr. Deepak Bhatnagar - ARS-USDA, New Orleans) under high humidity and under warm conditions. The inoculated corn contained $\sim$ 6250 ppb aflatoxin. Aflatoxin quantification was performed by the Office of the Texas State Chemist using high-performance liquid chromatography (HPLC). The corn were ground and mixed to form a single aflatoxin contaminated corn source for the feed experiment.

Aflatoxin-feed and clean-feed were prepared at the same ratios of corn, soybean and nutrients. The mixture was homogenized using horizontal rotary mixer for 12 minutes. The clay powders were incorporated into the feed during the mixing. Clays were added at 0.5% level (weight of the feed). The final concentrations of aflatoxins in the feed were analyzed by the Office of the Texas State Chemist. The aflatoxin concentration in the control feed (clean corn) was <20 ppb and, aflatoxin feed contained 1400 ppb. High aflatoxin concentration in the feed (>1000 ppb) is needed to cause significant alteration that can be detected by differences in body-weight (Aletor et al., 1981; Ostrowski-Meissner, 1984).

2.2.2 Feeding experiment

The poultry experiment consisted of an aflatoxin group (1400 ppb) and a clean corn group (<20 ppb). Each group was divided in three treatments: 1) no clay, 2) clay 4TX and 3) clay 1TX. Each treatment had 8 replicas with 5 chickens perreplica, for a total of 240 chickens. The clean feed group or control group was used to identify any potential negative effects caused by the clays in the feed. Meanwhile the aflatoxin group evaluated the efficacy of selected clays to adsorb aflatoxin before it can be assimilated by the organism.

3 Results

3.1 Characterization of bentonites as aflatoxin adsorbents

3.1.1 Aflatoxin adsorption

Sample 4TX showed a high adsorption capacity in the unfractionated sample and the clay fraction, while sample 1TX had moderate aflatoxin adsorption (Table 1) (Fig. 1). The lower aflatoxin adsorption of sample 1TX can be

attributed to dilution due to the greater silt content than 4TX. Additionally the XRD patterns indicated that opal CT was present inthe clay fraction of 1TX contributing to the dilution effect.

The clay fractions demonstrated a nearly linear isotherm curves (Fig. 1), which resulted in high adsorption capacities values that were not realistic (Table 1). The isotherms did not reach a plateau at the concentrations tested due to incomplete saturation of the adsorption sites on the clay. Moreover the affinity values indicated that aflatoxin accessibility to the interlayer was restricted. The drastically difference in adsorption capacities between the unfractionated samples and the clay fractions was a result of the exchangeable cation. The unfractionated materials were dominated by Ca whereas the clays were mostly Na saturated due to the fractionation treatments. The highest adsorption in both sample was observed in the Ca-saturated clays. Recent FTIR experiments showed that divalent and monovalent cations caused major shifts in the aflatoxin bands. These observations led to recent unpublished experiments which demonstrated that the cation valence and hydration energy affects the adsorption efficiency of the smectite clays.

3.1.2 Stability of adsorbed aflatoxin to clays

Two points of the isotherm were selected for the desorption experiment. Although different isotherm concentration points were used for each sample the data show that the clays even adsorbed more aflatoxin during the first wash, and no or negligible (<0.5%) desorption occurred in subsequent three washes. This desorption study suggested that the adsorbed aflatoxin is stable in the smectites. Both samples of each clay showed more than 10% of aflatoxin readsorbed from the solution (Fig. 2). The resistance of aflatoxin molecules to desorption was also confirmed by the constant concentration after the second to third wash (Fig. 2).

3.1.3 Ocurence of intelayer aflatoxin adsorption

Comparison of changes in the basal spacing of smectite was used to confirm the interlayer allocation of aflatoxin molecules. The Na-saturated clays without aflatoxin showed a basal spacing of 12.0 Å at room humidity (66%) and a reduced 10.0 Å at 0% humidity (N2 purge) (Fig. 3). Clays adsorbed aflatoxin showed an expansion of the smectite basal spacing to 14.0 Å at room humidity (66%), and to 13.0 Å under 0% humidity (Fig. 3). The aflatoxin adsorbed clays did not collapse to 10 Å after repeated N_2 purge. The higher basal spacing in the aflatoxin adsorbed clays confirmed that aflatoxin molecules were held in the interlayer space of these two samples.

3.1.4 Mineralogical composition

Both samples contained approximately the same percentage of sands (about 4%); sample 1TX had a higher percentage of silts (30.4%) than sample 4TX

(8.8%). The percentage of clay was greater in 4TX (87.6 %) than in 1TX (65.7%). The mineral composition of the unfractionated samples was dominantly smectite, and mostly concentrated in the clay fraction (Fig. 4). The broad reflections at $\sim$ 12.0 Å in the sand and silt fractions were due to Na-saturation of smectite by sodium acetate during sample treatment. These reflections were more prominent in sample 1TX, which indicates more clay remained in this sample fractions than in sample 4TX.

Quatz was present in both samples and concentrated in the sand and silt fraction (3.33 Å and 4.26 Å)(Fig. 4 and 5). Feldspars were also identified in both samples. Alkali feldspars, K-feldspar and albite occurred in sample 4TX, while plagioclase and orthoclase were present in sample 1TX. Biotite was the mineral identified by the presence of $\sim$ 10.0 Å (001) reflection and the lack of (002) reflection at 5.00 Å in the sand and silt fractions of both samples (Fig. 8b). Minor amount of muscovite was identified in the silt fraction of 4TX by its weak 5.00 Å reflection. Clinoptilolite was present in sample 4TX and concentrated in the silt fraction (8.9 Å)(Fig. 4).

The unfractionated 1TX showed 7.5 Å, and 4.28 Å XRD reflections, indicating the presence of gypsum, which was consistent with the high EC reading. This reflection disappeared in the sand and silt as gypsum was dissolved during the sample treatment (Fig. 5). Sample 1TX also contained pyrite, identified in the unfractionated material and concentrated in the silt fraction (Fig. 8a).

Montmorillonite was the dominant mineral in the clay fraction as indicated by the XRD of the Mg-glycerol treated samples (Fig. 7). Additionally the XRD showed the presence of opal-CT in the clay fraction of sample 1TX.

The FTIR spectra confirmed the presence of montmorillonite in the clay fraction. The strong band at 3626 cm^{-1} was attributed to the stretching vibration of OH groups in the octahedral sheets, indicating that Al^{3+} was the dominant cation in the octahedral sheets (Fig. 6) (Madejová, 2003), thus both samples are mainly dioctahedral. The isomorphic substitution resulted in OH bending bands in the range from 950 to 800 cm^{-1}. The bands at 919 (4TX) and 917(1TX) cm^{-1} were designated to the AlAl-OH bending vibrations. The band at $\sim$ 885 cm^{-1} was due to $Al^{3+}Fe^{3+}$-OH (Gates, 2005). In sample 4TX, the 885 cm^{-1} band was well defined while in sample 1TX it occurred only as a shoulder, which indicated more Fe present in the octahedral sheet of smectite in sample 4TX. The $\sim$ 845 cm^{-1} band was designated to the Al^{3+} Mg^{2+}-OH bending vibration.

Montmorillonite was assumed to be responsible for aflatoxin adsorption and it was concentrated in the clay fraction (as shown by XRD). Thus, other minerals are considered as diluents, and it is expected that high-clay content samples should have higher aflatoxin adsorption capacity.

Bentonites are composed of montmorillonite but other minerals are associated with it too. It is important to know the composition of the clays that are introduced to the animal feed in order to identify or avoid the inclusion of minerals or elements that can interfere with the animal health. Quartz and feldspars are mostly inert minerals and their chemical composition does not represent a risk for animals. These are common minerals found in soils and it

has been reported that several animal species tend to eat soil. Additionally the acid conditions in the stomach and the short residence time may not alter the stability of these minerals. In sample 1TX the presence of pyrite could be a concern but the reduced conditions of the intestinal tract favor its stability.

3.2 In vivo poultry experiment

3.2.1 Body weight of individual chickens

To compare the average body weight after 3 weeks, an ANOVA F-test was used following a complete randomized design (CRD) data analysis. The average body weights of chickens in <20 ppb aflatoxin treatment did not show significant differences. Although statistically it was not relevant, a slight decrease in average body weight in the clay treatments in comparison with no clay treatment was observed. This represents about 6.4 and 6.6 percent of reduction in clay 4TX and clay 1TX treatments, respectively. Similar weight reduction under clay treatments had been observed in other animal experiments (Kubena et al., 1993a; Bailey et al., 2006) but the explanation for this result was not addressed. The 0.5% addition of clay to the diet represents a same percentage of reduction in nutrient density, which can affect body weight. Additionally, due to the high adsorptive capacity of smectites there is a potential of the clays adsorbing some essential nutrients, which will be further tested. In the literature Zn, Mn, vitamin A and riboflavin had been evaluated as indicators of nutrient utilization, showing that at 0.5% clay addition did not cause significant impact (Phillips et al., 1995).

The difference in body weight of chickens under aflatoxin without clay diet was statistically different from the chickens subjected to aflatoxin plus clay treatments (Table 3). The addition of clay in the diet showed an increase in body weight, which reflects a 21% and 14% improvement with clay 4TX and clay 1TX, respectively. There was no significant difference among the clay treatments, suggesting that the clay effect was similar. The higher body weight in chickens under aflatoxin plus clay was an indirect indicator that the clays protected the animals from the toxic effects of the toxin.

The in vitro experiments showed that both clays were effective in adsorbing aflatoxin as also observed in the animal experiment. Moreover the experimental data showed that bentonite 4TX had a higher aflatoxin adsorption capacity than 1TX. This trend was also observed in the body weight of the chickens under aflatoxin plus clay feed. Even though there was no statistical difference between the average body-weight among the clay treatments, sample 4TX showed an increase in body weight of 21% while 1TX only increased the body weight by 14%. In the present study the in vitro result are in agreement with the in vivo performance in confirming the high binding capacity of the samples but also in the difference in adsorption. The characterization of the selection criteria is based only in bentonites samples and may not apply to other type of adsorbents.

3.2.2 Relative organ weight

The <20 ppb aflatoxin group showed no differences in any of the organ/body weight ratios, this observation indicates that the addition of clays in the diet did not cause significant secondary effects (Table 4). One of the most characteristic signs of aflatoxicosis is the deterioration or alteration in size and color of the liver, as a result of continuous exposure due to metabolic transformation of the aflatoxin molecules. In animal experiments with broiler chickens researcher observed an increase in relative liver weight of the animals on aflatoxin diet in comparison with the control group (Aletor et al., 1981; Huff et al., 1992; Jaraprakash et al., 1992; Bailey et al., 2006; Tessari et al., 2006).

However, in the present experiment, the liver/body weight ratio was not significantly different among treatments for the aflatoxin group. The similar ratios among the aflatoxin treatments could be a result of the high dose of aflatoxin in the diet. This indicates that the relative liver weight was not a sensitive parameter to show the protection effect of the clays, at $p<0.05$. Similar results were obtained by Bailey et al. (2006), where the addition of 0.5% of HSCA clay to a feed containing $\sim$ 3600 ppb of aflatoxin did not show significant differences in relative liver weight.

Researchers have observed that besides the liver other organs as heart, kidney, and spleen can be affected by aflatoxicosis, mainly by an increase in relative weight (Huff et al., 1992; Bailey et al., 1998; Quezada et al., 2000). Heart, kidney, and spleen weights were not significantly different among groups, indicating that these are not sensitive parameter to evaluate efficacy of the clays at a 5% level. This is in agreement with other animal experiments (Santurio, 1999). Tessari et al. (2006) observed differences in heart relative weight of animals subjected to different aflatoxin concentration; but no changes were observed in spleen relative weight.

3.2.3 Liver appearance

Livers from animals subjected to $<$ 20 ppb aflatoxin diet with and without clays had a similar dark red color and minimal size difference. In contrast, the high-aflatoxin exposure produced a significant change in the color of the livers with and without clay. Representative livers from animals under high aflatoxin without clay treatment showed pale yellow livers. The color improvement in the livers of animals feed with high aflatoxin plus clay treatment; indicating that less aflatoxin was gastro intestinally adsorbed. This indicates that the clays had a protective effect on the chickens by reducing the exposure.

The observations in this experiment concerning color differences in livers were in agreement with other animal experiments (Aletor et al., 1981; Phillips et al., 1988; Leeson et al., 1995; Miazzo et al., 2005). Aletor et al. (1981) had reported that the relative liver weight tends to increase in size due to the fat accumulation.

3.2.4 Aflatoxin level in liver

No aflatoxin was detected in livers from the <20 ppb aflatoxin clean feed treatment. Concentrations for the five aflatoxins tested were observed in the tissue samples on 1400 ppb aflatoxin contaminated feed (Table 5). AfB1 and AfG1 were present in the highest concentrations. These two are also the major forms present in the feed, and are metabolized to AfB2, AfG2 and AfM1. The metabolites are easily excreted, which explains the low concentrations observed (Chen et al., 1984). On the other hand the high levels of AfB1 and AfG1 were also indicators of overexposure because the livers were not able to metabolize all the mycotoxins absorbed.

Only AfB1 and AfG1 showed significant differences between the no clay and clay treatments. Considering the concentrations of all five aflatoxins, the total aflatoxin showed noticeable difference between the treatments (Table 5). The tissues from chicken subjected to an aflatoxin diet without clay addition showed higher concentration of total aflatoxin. There was a significant reduction (36%) in the total aflatoxins concentration by the addition of clay in the diet. The total aflatoxin concentration was similar for both clay treatments.

An important observation regarding the influence of AfB1 metabolism and high concentration in the liver was made by Chen et al. (1984). They conducted a similar experiment using high concentration of AfB1 (2057 ppb) but the levels in liver tissue was less than the reported in the present experiment. Based on the observation from previous experiments, they attribute that there is influence of the presence of AfG1 in the metabolism of AfB1 which affects the concentrations in the liver. This indicates that the source of aflatoxin in the feed can also affect the variability of the results, an important consideration for further studies.

3.3 Conclusions

The high clay content dominated by montmorillonite explains the high aflatoxin adsorption capacity of the bentonites. The different adsorption values can be attributed partially to the greater dilution of the smectite by the presence of other minerals in the sand and silt fraction but also in the clay. The diluent minerals (quartz, feldspars, mica) are common in soils and are unlikely to cause adverse effects on animals. Detailed characterization of the samples can reveal the presence of mineral and/or heavy metals that can interfere with the animal health.

Analysis of the adsorption capacity of the clay fraction confirmed the strong interlayer adsorption of aflatoxin molecules, which was resistant to washing. Yet the amount of aflatoxin that can be adsorbed was influenced by the dominant exchangeable cation. The divalent cation as Ca^{2+} in the unfractionated material offered better conditions for aflatoxin adsorption than Na^{+} in the clay fraction.

The in vivo experiments showed that both clays were effective in adsorbing aflatoxin. Bentonite 4TX increased more the body weight and both bentonites reduced concentrations of aflatoxins in liver. The better performance of clay 4TX is in agreement with the in vitro experiment presented in previous chap-

ters. Additionally, chickens subjected to an aflatoxin plus clay diet showed an improvement in liver color. Despite the improvements, the chickens fed bentonite did not have a 100% recovery from aflatoxin toxicity.

References

Aletor, V. A., Kasali, O. B., and Fetuga, B. L. (1981). Effects of sublethal levels of dietary aflatoxins in broiler chickens. *Zentralblatt fr Veterinrmedizin Reihe A*, 28(9-10):774–781. 10.1111/j.1439-0442.1981.tb01250.x.

Arafa, A., Bloomer, R., Wilson, H., Simpson, C., and Harms, R. (1981). Susceptibility of various poultry species to dietary aflatoxin. *British Poultry Science*, 22:431–436.

Bailey, C. A., Latimer, G. W., Barr, A. C., Wigle, W. L., Haq, A. U., Balthrop, J. E., and Kubena, L. F. (2006). Efficacy of montmorillonite clay (novasil plus) for protecting full-term broilers from aflatoxicosis. *Journal of Applied Poultry Research*, 15(2):198–206.

Bailey, R., Kubena, L., Harvey, R., Buckley, S., and Rottinghaus, G. (1998). Efficacy of various inorganic sorbents to reduce the toxicity of aflatoxin and t-2 toxin in broiler chickens. *Poultry Science*, 77(11):1623–1630.

Chen, C., Pearson, A. M., Coleman, T. H., Gray, J. I., Pestka, J. J., and Aust, S. D. (1984). Tissue deposition and clearance of aflatoxins from broiler chickens fed a contaminated diet. *Food and Chemical Toxicology*, 22(6):447–451. doi: DOI: 10.1016/0278-6915(84)90327-2.

Dalvi, R. (1986). An overview of aflatoxicosis of poultry: its characteristics, prevention and reduction. *Veterinary Research Communications*, 10(1):429–443.

Huff, W. E., Kubena, L. F., Harvey, R. B., and Phillips, T. D. (1992). Efficacy of hydrated sodium calcium aluminosilicate to reduce the individual and combined toxicity of aflatoxin and ochratoxin-a. *Poultry Science*, 71(1):64–69.

Jaraprakash, M., Gowda, R., Vijasarathi, S., and Seshadri, S. (1992). Adsorbent efficacy of hydrated sodium calcium aluminosilicate in induced aflatoxicosis in briolers. *Indian Journal of Veterinary Pathology*, 16:102–105.

Jouany, J. P. and Diaz, D. (2005). *Effects of mycotoxins in ruminants*, pages 295–299. Nottingham University Press, Nottingham.

Kermanshashi, H., Hazegh, A., and Afzali, N. (2009). Effect of sodium bentonite in broiler chickens fed diets contaminated with aflatoxin b1. *Journal of Animal and Veterinary Advances*, 8(8):1631–1636.

Kubena, L. F., Harvey, R. B., Huff, W. E., and Corrier, D. E. (1990). Efficacy of a hydrated sodium calcium aluminosilicate to reduce the toxicity of aflatoxin and t-2 toxin. *Poultry Science*, 69:1078–1086.

Leeson, S., Diaz G, G. J., and Summers, J. D. (1995). *Poultry metabolic disorders and mycotoxins*. University Books, Ontario, Canada.

Lindemann, M. D., Blodgett, D. J., Kornegay, E. T., and Schurig, G. G. (1993). Potential ameliorators of aflatoxicosis in weanling growing swine. *Journal of Animal Science*, 71(1):171–178.

Madejová, J. (2003). Ftir techniques in clay mineral studies. *Vibrational Spectroscopy*, 31(1):1–10. doi: DOI: 10.1016/S0924-2031(02)00065-6.

Miazzo, R., Peralta, M., Magnoli, C., Salvano, M., Ferrero, S., Chiacchiera, S., Carvalho, E., Rosa, C., and Dalcero, A. (2005). Efficacy of sodium bentonite as a detoxifier of broiler feed contaminated with aflatoxin and fumonisin. *Poultry Science*, 84(1):1–8.

Pasha, T. N., Farooq, M. U., Khattak, F. M., Jabbar, M. A., and Khan, A. D. (2007). Effectiveness of sodium bentonite and two commercial products as aflatoxin absorbents in diets for broiler chickens. *Animal Feed Science and Technology*, 132(1-2):103–110. doi: DOI: 10.1016/j.anifeedsci.2006.03.014.

Phillips, T., Clement, B. A., and Park, D. L. (1994). *Approaches to reduction of aflatoxins in foods and feeds*, pages 383–399. Academic Press, Inc, San Diego, CA.

Phillips, T., Kubena, L. F., Harvey, R. B., Taylor, D. R., and Heidelbaugh, N. (1987). Mycotoxin hazards in agriculture: new approach to control. *Journal of Animal Veterinary Medicine*, (190):1617–1618.

Phillips, T. D. and Carpenter, R. H. (2008). Composition comprising calcium aluminosilicate clay and methods for the enterosorption and management of toxins. CAN 148:128308 63-6 Pharmaceuticals Patent 20080110 1305-78-8 (Calcium oxide (CaO); 1309-37-1 (Ferric oxide); 1309-48-4 (Magnesium oxide (MgO); 1313-59-3 (Sodium oxide); 1327-39-5 (Calcium aluminosilicate); 1344-28-1 (Alumina); 1344-43-0 (Manganous oxide); 7631-86-9 (Silica); 12136-45-7 (Potassium oxide) Role: THU (Therapeutic use), BIOL (Biological study), USES (Uses) (compn. comprising calcium aluminosilicate clay and methods for the enterosorption and management of toxins) 424489000. A1 US 2006-816824 20060627.

Phillips, T. D., Kubena, L. F., Harvey, R. B., Taylor, D. R., and Heidelbaugh, N. D. (1988). Hydrated sodium calcium aluminosilicate: a high affinity sorbent for aflatoxin. *Poultry Science*, 67:243–247.

Phillips, T. D., Sarr, A. B., and Grant, P. G. (1995). Selective chemisorption and detoxification of aflatoxins by phyllosilicate clay. *Natural Toxins*, 3:204–213.

Pimpukdee, K., Kubena, L. F., Bailey, C. A., Huebner, H. J., Afriyie-Gyawu, E., and Phillips, T. D. (2004). Aflatoxin-induced toxicity and depletion of hepatic vitamin a in young broiler chicks: protection of chicks in the presence of low levels of novasil plus in the diet. *Poultry Science*, 83(5):737–744.

Quezada, T., Cullar, H., Jaramillo-Jurez, F., Valdivia, A. G., and Reyes, J. L. (2000). Effects of aflatoxin b1 on the liver and kidney of broiler chickens during development. *Comparative Biochemistry and Physiology Part C: Pharmacology, Toxicology and Endocrinology*, 125(3):265–272. doi: DOI: 10.1016/S0742-8413(99)00107-3.

Ramos, A. J. and Hernandez, E. (1996). In vitro aflatoxin adsorption by means of a montmorillonite silicate. a study of adsorption isotherms. *Animal Feed Science and Technology*, 62(2-4):263–269.

Rosa, C., Miazzo, R., Magnoli, C., Salvano, M., Chiacchiera, S., Ferrero, S., Saenz, M., Carvalho, E., and Dalcero, A. (2001). Evaluation of the efficacy of bentonite from the south of argentina to ameliorate the toxic effects of aflatoxin in broilers. *Poultry Science*, 80(2):139–144.

Santurio, J. M. (1999). Effect of sodium bentonite on the performance and blood variables of broiler chickens intoxicated with aflatoxins. *British Poultry Science*, 40(1):115 – 119.

Tessari, E. N. C., Oliveira, C. A. F., Cardoso, A. L. S. P., Ledoux, D. R., and Rottinghaus, G. E. (2006). Effects of aflatoxin b1 and fumonisin b1 on body weight, antibody titres and histology of broiler chicks. *British Poultry Science*, 47(3):357 – 364.

Thieu, N. and Pettersson, H. (2008). Evaluation of the capacity of zeolite and bentonite to adsorb aflatoxin in simulated gastrointestinal fluids. *Mycotoxin Research*, 24(3):124–129.

Table 1: Aflatoxin adsorption isotherm values for unfractionated samples and clay fraction.

Sample	K_d	Qmax (ml/kg)	η^2
4TX Unfractionated	2.94 x 10^5	0.5784	0.987
1TX Unfractionated	4.39 x 10^5	0.4348	0.972
4TX Ca-Clay	6.98 x 10^5	0.5221	0.953
1TX Ca-Clay	2.65 x 10^5	0.5188	0.935
4TX Na-Clay	3.10 x 10^4	0.9717	0.993
1TX Na-Clay	0.8064	0.8073	0.979

Table 2: Treatments body weight per bird and FCR means comparison

Treatment	No. Birds	Body weight per bird	Feed Conversion ratio (FCR)
		Aflatoxin feed group	
Clay 4TX	31	$379^{a} \pm 5$	$0.600^{a} \pm 0.033$
Clay 1TX	30	$348^{ab} \pm 12$	$0.628^{a} \pm 0.023$
No Clay	30	$308^{b} \pm 14$	$0.536^{a} \pm 0.037$
		Clean feed group	
No Clay	40	$724^{A} \pm 15$	$0.562^{A} \pm 0.026$
Clay 4TX	40	$677^{A} \pm 24$	$0.526^{A} \pm 0.013$
Clay 1TX	40	$675^{A} \pm 22$	$0.508^{A} \pm 0.025$

Data in a group with differenct letters (^{ab}) are significanttly different at $p<0.05$

Table 3: Organ body weight ratio differences by group

Treatment	No. birds	Body weight (g)	Treatment comparison (α=0.05)	
		Aflatoxin feed group		*Improvement (%)*
Clay 4TX	31	371 ± 12	A	21
Clay 1TX	30	351 ± 12	B	14
No Clay	30	307 ± 11	B	control
		Clean feed group		*Reduction (%)*
No Clay	40	724 ± 15	A	control
Clay 4TX	40	678 ± 25	AB	6.4
Clay 1TX	40	675 ± 23	B	6.6

Data in a group with differenct letters (A B) are significanttly different at p<0.05

Table 4: Organ body weight ratio differences by group

Treatment	No. birds	Organ body weight ratio			
		liver	Spleen	Kidney	Heart
		Aflatoxin feed group			
Clay 4TX	31	0.0464^{ab}	0.0195^{a}	0.00234^{a}	0.00970^{a}
Clay 1TX	30	0.0489^{a}	0.0186^{a}	0.00230^{a}	0.00926^{a}
No Clay	30	0.0444^{a}	0.0179^{a}	0.00224^{a}	0.00970^{a}
		Clean feed group			
Clay 4TX	40	0.0327^{A}	0.0086^{A}	0.0011^{A}	0.0064^{A}
Clay 1TX	40	0.0323^{A}	0.0086^{A}	0.0010^{A}	0.0066^{A}
No Clay	40	0.0310^{A}	0.0079^{A}	0.0010^{A}	0.0064^{A}

(^{ab}) Data in a colum with differenct superscripts are significanttly different at p<0.05

Table 5: Aflatoxin concentration in livers from chickens in the high aflatoxin contaminated feed treatments

	concentration in liver (ppb)					
Treatment	AfB1	AfG1	AfB2	AfG2	AfM1	Total Aflatoxins
No Clay	18.8^{a}	16.4^{a}	0.30^{a}	1.18^{a}	1.34^{a}	38.02^{a}
Clay 4TX	14.6^{ab}	7.6^{b}	0.46^{a}	0.46^{a}	1.20^{a}	24.32^{b}
Clay 1TX	10.0^{b}	11.0^{ab}	0.18^{a}	2.00^{a}	0.86^{a}	24.04^{b}

(^{ab}) Data in a colum with differenct superscripts are significanttly different at $p<0.05$

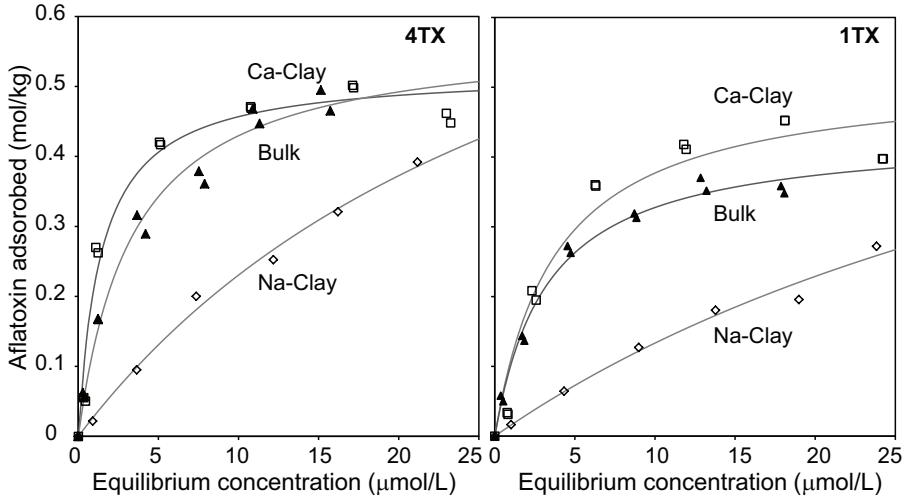

Figure 1: Adsorption isotherms of the unfractionated material and clay fraction of samples 4TX and 1TX.

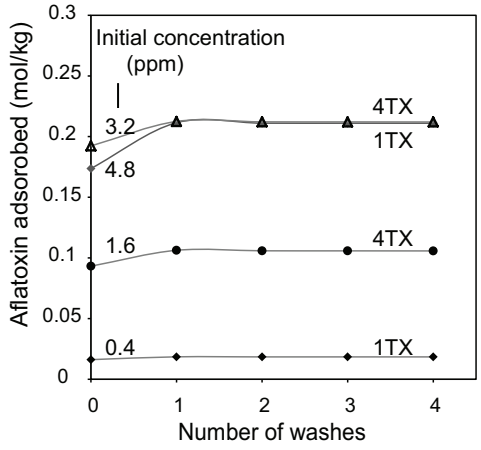

Figure 2: Aflatoxin desorbed after wasing with water.

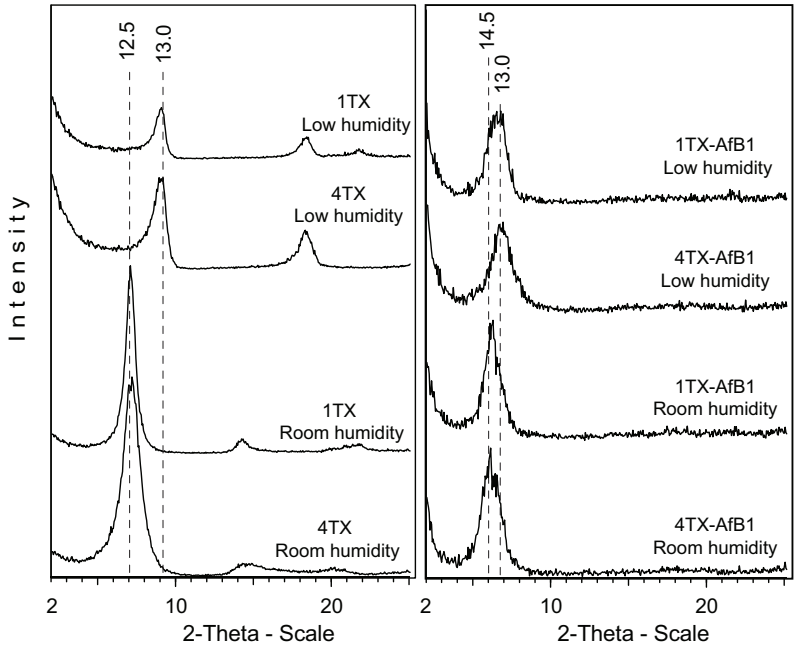

Figure 3: XRD patterns of Na-saturated clays from samples 4TX and 1TX with and without AfB1 at room and zero humidity.

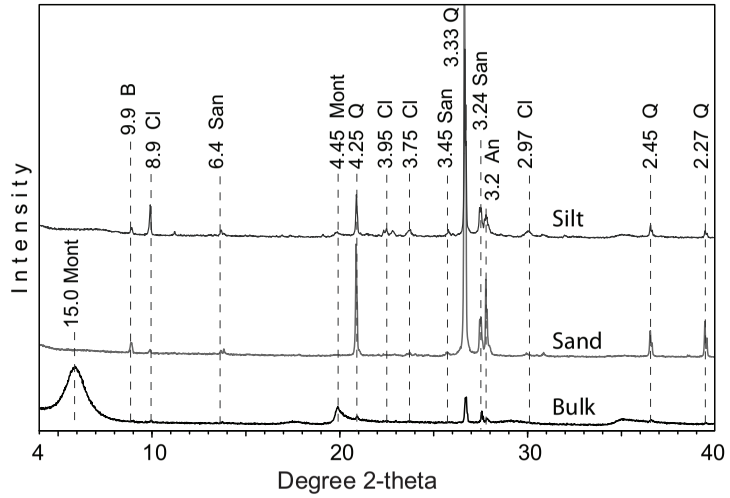

Figure 4: XRD patterns of bulk, sands and silts of sample 4TX.

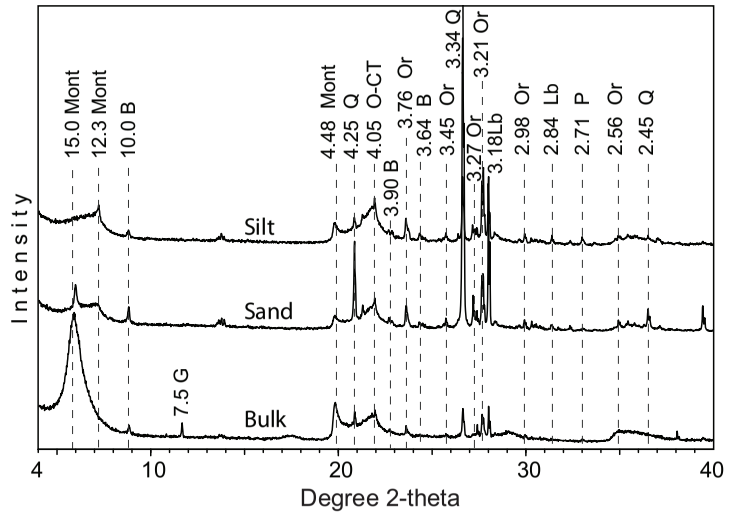

Figure 5: XRD patterns of bulk, sand and silts of samples 1TX.

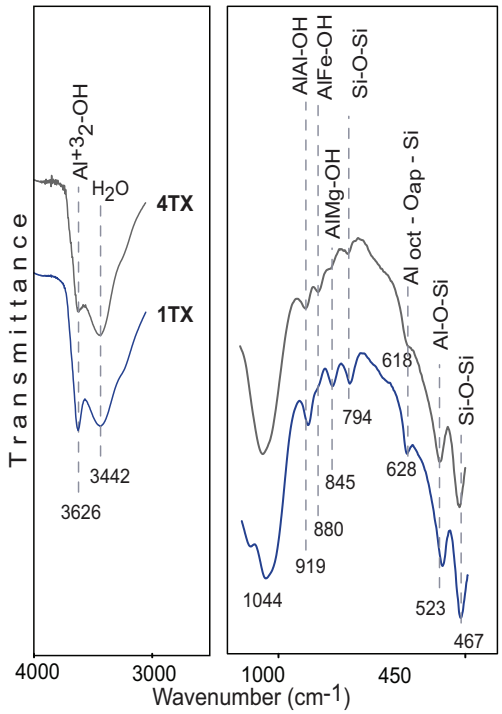

Figure 6: FTIR spectra of clay fraction.

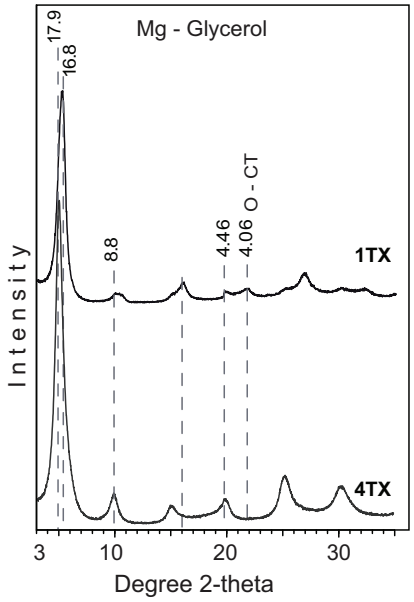

Figure 7: XRD patterns of clay fraction treatments.

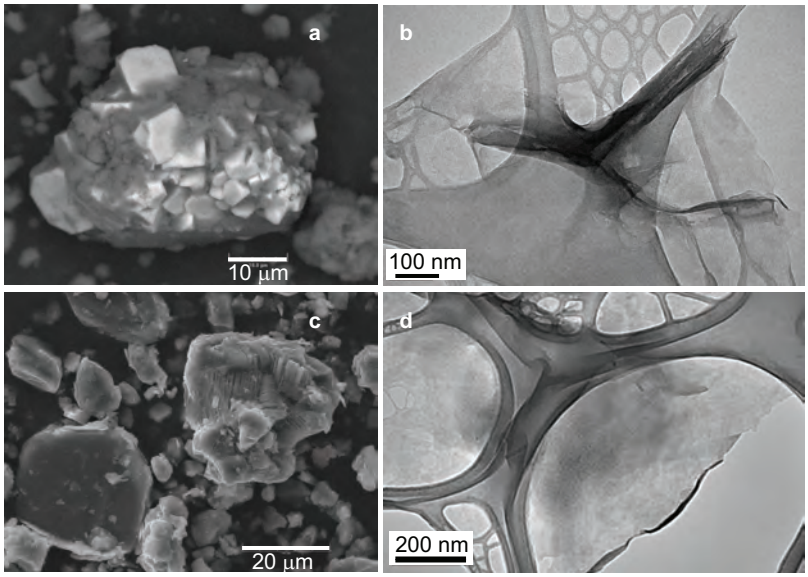

Figure 8: SEM images of silt fraction: a)Pyrite particle with smectite in sample 1TX, and c) 4TX. TEM images of the clay fraction: b)4TX and d)1TX.